Identification of HIV-Reservoir Cells with Reduced Susceptibility to Antibody-Dependent Immune Response

Antonio Astorga-Gamaza[1], Judith Grau-Expósito[1], Joaquín Burgos[1], Jordi Navarro[1], Adrià Curran[1], Bibiana Planas[1], Paula Suanzes[1], Vicenç Falcó[1], Meritxell Genescà[1], and Maria J. Buzon[1]*

[1]Infectious Disease Department, Hospital Universitari Vall d'Hebron, Institut de Recerca (VHIR), Universitat Autònoma de Barcelona, Barcelona, Spain.

Running title: Immune resistance of HIV-infected cells to NK-ADCC killing

Corresponding authors*: Maria J. Buzon (mariajose.buzon@vhir.org)

Abstract

HIV establishes a persistent infection in heterogeneous cell reservoirs, which can be maintained by different mechanisms including cellular proliferation, and represent the main obstacle to curing the infection. The expression of the Fcγ receptor CD32 has been identified as a marker of the active cell reservoirs in people on antiretroviral therapy, but if its expression has any role in conferring advantage for viral persistence is unknown. Here, we report that HIV-infected cells expressing CD32 have reduced susceptibility to natural killer (NK) antibody-dependent cell cytotoxicity (ADCC) by a mechanism compatible with the suboptimal binding of HIV-specific antibodies. Infected CD32 cells have increased proliferative capacity in the presence of immune complexes, and are more resistant to strategies directed to potentiate NK function. Remarkably, reactivation of the latent reservoir from antiretroviral-treated people living with HIV increases the pool of infected CD32 cells, which are largely resistant to the ADCC immune mechanism. Thus, we report the existence of reservoir cells that evade part of the NK immune response through the expression of CD32.

Graphical Abstract

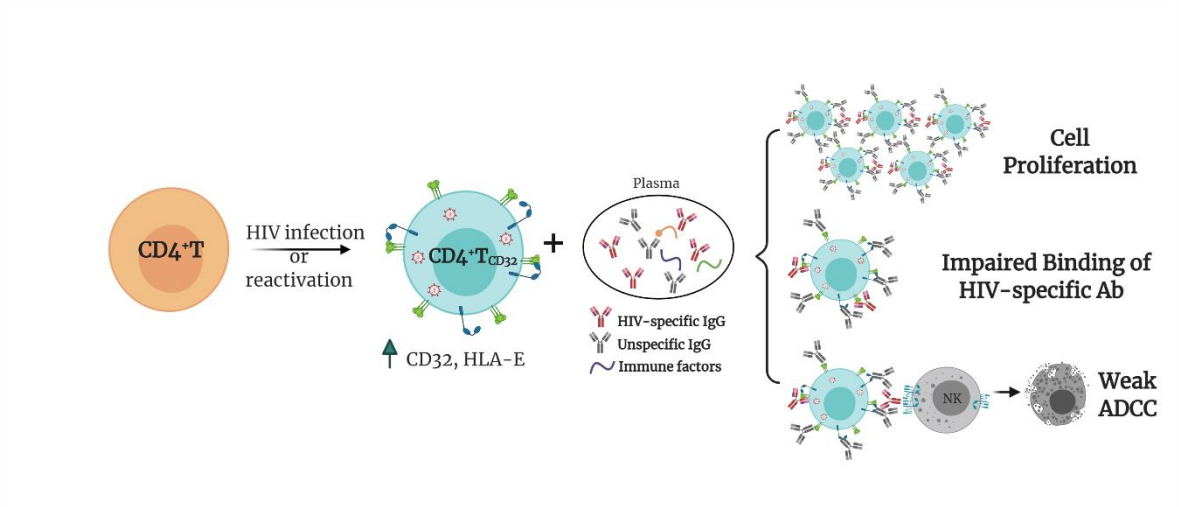

Introduction

Human immunodeficiency virus (HIV) establishes a persistent infection for which, nowadays, there is no available cure. Despite huge advances on the optimization of antiretroviral therapy (ART), which leads to suppression of viral replication, ART does not fully eliminate the virus from the human body nor can completely solve the persistent inflammation caused by HIV [1]. Importantly, ART discontinuation leads to viral rebound from diverse anatomical sites and cell subsets containing replication-competent virus, representing the main obstacle in achieving cure [2].

The HIV reservoir has a complex and heterogeneous nature, where each of the subsets that compose the viral reservoir contributes differently to viral persistence; i.e. central memory cells are the main population contributing to the total reservoir size [3], effector memory cells support HIV transcription [4], and memory stem cells and resident memory T cells are potentially long-lived niches for HIV [5, 6]. Unfortunately, knowledge on the establishment, maintenance, and composition of the reservoir remains incomplete, and the identification of markers to exclusively target persistent HIV-infected cells remains elusive [7, 8]. In this regard, the molecule CD32, a low-affinity receptor for the constant fraction of immunoglobulin G (FcγR-IIa), was proposed as a marker of HIV reservoir cells [9]. While those results were questioned later by the identification of experimental artifacts [10, 11], several new studies partially corroborated the original findings; higher levels of viral DNA within the T_{CD32} population were reported after applying a very stringent cell isolation protocol [12] and CD32 was identified as a marker of transcriptionally active persistent

HIV-infected cells, both in blood and in the main reservoir tissues, namely the lymph nodes and the gastrointestinal tract [6, 13-16]. Importantly, whether or not CD32 is a marker of latent or transcriptionally active infection, infected $CD4^+$ T cells expressing CD32 contain replication-competent HIV and are found in long-term ART-treated people living with HIV (PLWH) [6, 9, 12-15, 17, 18]. The cell markers CD20 [19] and CD30 [20] have been shown to also identify transcriptionally active HIV cells in samples from ART-suppressed PLWH. Whether these transcriptionally active HIV-infected cells persist in the body and are not targeted by host immune responses remains unknown.

Natural killer (NK) cells are lymphocytes that can eliminate cancer cells or virally-infected cells without prior antigen sensitization. They constitute an important arm of the immune system, not only by a direct cytotoxic effect on aberrant cells but also by the modulation of the adaptive immune responses. NK cells kill target cells by several mechanisms, such as natural cytotoxicity (NC), recognizing stress ligands expressed on the surface of infected cells, or by antibody-dependent cell cytotoxicity (ADCC), driven by antibodies that bind to target cells [21]. The decision of NK cells to kill or not to kill a target cell depends on the balance between activating and inhibitory signals received from the interaction with the target cell [22]. Among relevant NK receptors, we find natural cytotoxicity receptors such as NKp46, NKp30, NKp44, different Killer-cell immunoglobulin-like (KIRs), and lectin-like receptors such as NKG2A or NKG2C. Other important activating receptors for NK activity are NKG2D and DNAM-1, whose known ligands are the major histocompatibility complex (MHC) class I-related molecules MICA/B and the UL16-binding proteins or CD155 and CD112, respectively. Further, expression of the inhibitory receptor NKG2A is known to impact NK effector responses through its interaction with HLA-E molecules [23]. In this sense, therapeutic interventions blocking this interaction represent promising tools to potentiate NK cell immune responses during different pathologies [24, 25]. Importantly, HIV infection causes NK cell dysfunction, which is not completely restored by ART [26, 27]. NK cells play an important role in containing viral replication during early infection and shaping adaptive immune responses during chronic infection [28]. However, the role of NK cells in controlling the viral reservoir in PLWH on ART remains undefined. Mounting evidence supports the importance of NK cell function in shaping the HIV reservoir size, for example through the induction of interferon (IFN-ɣ) and the expression of certain activating receptors [29]. Moreover, proportions of NK cells inversely correlated with HIV-1 DNA reservoir levels in a clinical study designed to disrupt viral latency [30]. Importantly, during chronic infection, several strategies used by HIV to evade NK cell immune responses have been described, including the modulation of HLA class I molecules expression at the surface of infected cells [31]. However,

immune evasion mechanisms of HIV-infected reservoir cells to NK cell-mediated killing have not been identified.

Here we show that CD32 expression on HIV-infected cells confers a reduced susceptibility to NK cell-mediated ADCC killing by a mechanism compatible with a reduced binding of HIV-specific antibodies required for this mechanism. Importantly, this immune-resistant mechanism is also observed in latently HIV-infected cells from ART-treated PLWH after viral reactivation, providing a plausible explanation for the maintenance of transcriptionally active HIV-infected cells in ART-treated PLWH.

RESULTS

Susceptibility of HIV-reservoir cell subsets to NK immune response

While it is clear that ADCC, largely mediated by NK cells, is an important protective mechanism against HIV and SIV infection [32-34], the capacity of this immune mechanism to limit the infection of different T cell subsets composing the viral reservoir is currently unknown. Thus, we first assessed the intrinsic susceptibility of Naïve (T_{NA}), Stem Cell Memory (T_{SCM}), Central Memory (T_{CM}), Effector Memory (T_{EM}), T_{CD20}^{dim}, and T_{CD32}^{dim} $CD4^+$ T cell subsets to ADCC response. Gp120 coated $CD4^+$ T cells from 15 ART-treated and virologically-suppressed PLWH (participants #8-22, **Table S1**) were subjected to a flow cytometry-based ADCC assay [35]. In this assay, we used gp120-coated cells and plasma from an HIV-infected person with a high titer of HIV-specific immunoglobulins, which allowed a comparative evaluation of the intrinsic susceptibility of the different subpopulations to NK-mediated killing. Gating of CD32 cells was performed as previously reported in our previous publications [13, 6], whereby possible contaminant cell conjugates with monocytes or B cells (defined as $CD4^+$ $CD32^{high}$ cells), were excluded. Coating efficiency with the recombinant protein gp120 of different cell subsets is shown in **Figure S1A**, and a representative gating strategy used for the identification of killed cells by ADCC is shown in **Figure S1B**. Results showed that each $CD4^+$ T cell subset had a different susceptibility to autologous NK cells, being T_{EM}>T_{CM}> T_{CD20}^{dim}>T_{NA}>T_{SCM}>T_{CD32}^{dim} more prone to be killed (ANOVA Friedman test p=0.0001) (**Figure 1A**). Overall, most $CD4^+$T cell subsets were susceptible to ADCC, however T_{CD32}^{dim} cells, and to a lesser extent T_{SCM}, showed the highest resistance to ADCC.

To address if the pattern observed for CD32 cells was exclusive of ART-treated PLWH, we included samples from Elite controllers (EC) and healthy donors (HD). First, we compared the expression of CD32 in $CD4^+$ T cells in the three cohorts (participants #1-22, **Table S1**), following a very stringent flow cytometry gating strategy (**Figure S1B**). In agreement with previous studies [12, 13, 36, 37], we found that a median of 1.21% of $CD4^+$ T cells expressed the CD32 receptor, and no statistically significant differences were detected between ART-suppressed, EC participants and HD (**Figure S1C**). In addition, and in concordance with the study of García et al., but differing from the report of Darcis et al. [12, 37], there was no correlation between the HIV-DNA or HIV-RNA levels and the frequency of CD32 expression on $CD4^+$ T cells (**Figure S1D and S1E**). We then performed the NK-ADCC assays. We observed that overall, NK cells from healthy donors were highly efficient at killing the total $CD4^+$ T cell population (**Figure 1B**) and the different $CD4^+$ T subsets (**Figure 1C**). EC represented a heterogeneous group of individuals, in which no significant differences were detected compared to HD as a total (**Figure 1B**) or by subset (**Figure 1C**). In contrast, total $CD4^+$ T cells (**Figure 1B**) as well as all subsets from ART-treated PLWH were less susceptible to ADCC-mediated killing than HD (**Figure 1C**). The altered frequencies, phenotypes, and decreased functions of NK cell subsets reported during HIV infection [38], which are not fully restored by ART [27], could explain the different NK potency observed in these ART-suppressed PLWH. Notably, and regardless of that, NK cells from all cohorts showed a marked impaired capacity to kill T_{CD32}^{dim} cells (median % of ADCC of 0.00, 34.84, and 45.01, for ART, EC, and HD, respectively) (**Figure 1C** and **Figure S1F and S1G**). We also investigated the potential relationship between the total cell reservoir size in vivo and ADCC activity. We observed a statistically significant inverse correlation between the percentage of ADCC activity against $CD4^+$ T cells and the total HIV-DNA reservoir size (**Figure 1D**) and, in particular, for the ADCC against T_{CD32}^{dim} cells (**Figure 1E**).

HIV proteins are known to alter the expression of molecules on the infected cells, thereby impacting their recognition and likely the killing mediated by immune cells. Thus, we ought to confirm our results in a more physiological setting using ex vivo infected $CD4^+$ T cells. Isolated $CD4^+$ T cells from ART-suppressed PLWH were infected with HIV_{BaL} or $HIV_{NL4.3}$, and after 5 days, were subjected to NK natural cytotoxicity (NC) and ADCC assays (participants #23-29, 36, 44, 46-49 and 51, **Table S1**). A representative flow gating strategy is shown in **Figure 1F.** After the ex vivo infection, we observed higher expression of the CD32 molecule in comparison to uninfected cells (**Figure S2A and S2B**). Moreover, no significant differences between the killing of T_{CD32}^{dim} and T_{CD32}^{neg} by NC in ART-suppressed PLWH were observed (**Figure 1G**). However, and in concordance with results in

Figures 1A and **C**, T_{CD32}^{dim} cells from ART-suppressed PLWH were significantly more resistant to ADCC in comparison to their negative cell counterparts (median % ADCC killing normalized to NC of 19.66 vs 35.85 for T_{CD32}^{dim} and T_{CD32}^{neg}, respectively) (**Figure 1H**). In addition, we observed that the capacity to kill infected T_{CD32}^{dim} cells was directly related to the global capacity to kill all infected cells, indicating the essential role of NK potency, in addition to the intrinsic susceptibility of the target cells (**Figure S2C**). These results show that, regardless of differences between individuals on the overall killing capacity of their NK cells, different subpopulations of infected $CD4^+$ T cells have distinct intrinsic susceptibility to ADCC responses, being the pool of $CD4^+$ T cells expressing the CD32 molecule more resistant. Moreover, ART-suppressed individuals, most likely due to the existence of impaired NK cells, have a remarkable inability to kill this population of infected cells.

Viral-reactivated cells expressing CD32 from ART-treated PLWH are resistant to NK cell-mediated cytotoxicity.

Next, we examined if this NK-resistant profile might also affect the latent reservoir after viral reactivation. First, using samples from 9 ART-suppressed PLWH (subjects #59-67, **Table S1**), we reactivated $CD4^+$ T cells with different latency-reversing agents (LRA) and applied the Prime Flow RNA (FISH-flow) *in situ* hybridization (ISH) assay, which allows detecting at a single cell level cells expressing viral RNA, as described before [39, 40]. The gating strategy is shown in **Figure S3A**. We observed a higher increase of HIV-RNA^+ cells in the T_{CD32}^{dim} fraction compared to T_{CD32}^{neg} cells in all conditions and, within T_{CD32}^{dim} cells, HIV-RNA^+ cells were more frequent after LRA treatment compared to untreated cells (**Figure 2A**). Upregulation of CD32 expression upon the treatment with several LRAs was evidenced in total $CD4^+$ T cells (**Figure S3B**). Furthermore, we performed functional NK assays using samples from 22 additional ART-suppressed PLWH after reactivation of the natural HIV reservoir (participants #68-89, **Table S1**). First, we evaluated viral reactivation by intracellular p24 (**Figure S3C**) and successfully observed viral reactivation of dormant HIV in 17 of these samples (**Figure 2B**). An example of p24 detection using this functional assay is shown in **Figure S3D**. Also in line with our previous results, we found a higher frequency of viral reactivated cells ($p24^+$ cells) within the T_{CD32}^{dim} fraction (**Figure 2C**). After the NK killing assays, viral-reactivated cells, in general, were susceptible to ADCC (**Figure 2D**, NK + plasma condition). Of note, we used autologous plasma from the same virologically-suppressed PLWH (mean time of undetectable viremia of 60 months [range 25-118]). This is noteworthy since ART treatment may decrease the number of antibodies mediating ADCC [41]. We next evaluated the population of viral-reactivated cells expressing CD32

in these PLWH. We observed an increase in the expression of CD32 after latency disruption, which constituted a significant fraction of the total pool of viral reactivated cells (**Figure 2E**). Remarkably, this population was refractory to ADCC and even increased after the ADCC assays (condition with plasma) (**Figure 2F**). Thus, concordantly with previous results, T_{CD32}^{dim} cells showed a higher pattern of ADCC resistance compared to the total HIV-reactivated cells (**Figure 2G**). Altogether, our results show that the latent HIV reservoir expresses CD32 upon viral reactivation with LRAs, and the resulting T_{CD32}^{dim} infected cells are less sensitive to NK-mediated ADCC killing than the whole infected population. Importantly, antibodies endowed with ADCC-triggering capacity are still present in some ART-suppressed PLWH, yet the T_{CD32}^{dim} population might escape from this immune mechanism.

Infected T_{CD32}^{dim} cells expressing activating or inhibitory NK ligands are refractory to NK-mediated killing

To ascertain if differences in receptor-ligand interactions could be responsible for the impaired capacity of the NK cells to kill the T_{CD32}^{dim} subset, we studied the expression of MICA/B, ULBP-1, CD155, and HLA-E on the surface of HIV-infected cells after ex vivo infection. Of note, the impact of HIV infection on the expression of many of these ligands is not fully understood and seems to depend on the viral strain and the stage of the viral infection [42, 43]. Expression of the ligands was assessed by flow cytometry, and the gating strategy used for these analyses is shown in **Figure S4A**. Overall, we observed that, despite HIV induced higher expression of MICA/B, ULBP-1, and CD155 in infected cells compared to uninfected cells, only a small proportion of infected cells expressed these activating ligands (**Figure 3A and B**). In contrast, the ligand HLA-E was found to be expressed in a significantly higher proportion of infected cells (median of 12.0% in HIV-infected cells vs. 9.4% in uninfected cells, p=0.002) (**Figure 3C and D**). By analyzing infected cells based on their expression of CD32, the same trend was observed for the receptors MICA/B, ULBP1, or CD155 (median 0.6%, 1.28%, 0.37% for infected T_{CD32}^{dim} vs. 0.26%, 0.09%, 0.26% for the infected T_{CD32}^{neg} fraction) (**Figure 3E and F**). However, HLA-E expression was 2-fold significantly higher in HIV-infected T_{CD32}^{dim} compared to infected T_{CD32}^{neg} cells (median of 22.2% and 11.0% respectively, p<0.0001) and differences in MFI were also detected (**Figure 3G and H**). Of note, in the absence of any viral infection, T_{CD32}^{dim} cells showed intrinsically higher HLA-E expression (**Figure S4B**).

Next, we ought to determine the expression of activating and inhibitory ligands on the fraction of cells refractory to ADCC after ex vivo infection. We performed both NC and ADCC functional

assays (in cells from participants #36, 40, 44, 45, 47-49, and 51, **Table S1**). The infected population ($p24^+$) expressing the ligand ULBP-1 was significantly eliminated by both mechanisms, NC and ADCC (**Figure 3I**), however infected cells expressing MICA/B and CD155 were only eliminated by NC (**Figure 3J and K**). Of note, as previously reported [25, 44], cells expressing the molecule HLA-E were particularly resistant to NK-mediated killing (**Figure 3L**). However, infected T_{CD32}^{dim} cells expressing any of the activating NK ligands were more refractory to both NK-mediated immune responses (**Figure 3M-P**). Overall, we observed that upon HIV infection, target cells expressing NK-activating ligands were susceptible to natural cytotoxicity mediated by NK cells. However, infected cells expressing HLA-E and, particularly, $CD32^{dim}$ cells expressing this molecule and/or the activating ligands MICA/B, ULBP-1, and CD155, were more resistant to NK-mediated killing.

Suboptimal binding of HIV-specific immunoglobulins to CD32 in HIV-infected cells inefficiently triggers NK cell degranulation

Different hypotheses might help to explain why T_{CD32}^{dim} cells are more resistant to ADCC. CD32a is a low-affinity receptor for the constant fraction of immunoglobulin G (FcγR-IIa) [45-47], and the expression of this molecule on HIV-infected cells would provide them with a bivalent capacity to interact with immunoglobulins present in plasma, both through their constant fraction (Fc portion) or the variable fragment (antigen-specific). In addition, pentraxins, conserved innate immune molecules involved in infectious processes and inflammation, can bind to CD32 and compete with IgGs [48]. Thus, the engagement of such molecules or immune complexes (IC) to the CD32 Fc receptor might offer a selective advantage by protecting infected cells from HIV-specific ADCC-inducing antibodies. Accordingly, we tested if HIV-specific immunoglobulins (Igs) were able to efficiently bind to CD32-expressing cells previously coated with gp120. After incubation with plasma containing HIV-unspecific immunocomplexes (ICs), we found a decrease in the total number of HIV-specific molecules (A32 mAb) able to bind to T_{CD32}^{dim} cells (**Figure 4A-B**), but such effect was not observed in the T_{CD32}^{neg} population (**Figure 4C**). A reduction in the total number of cells being recognized by the A32 mAb was not observed (**Figure S5A-B**). This suggests that components present in plasma might bind to the FcγR receptor CD32 representing a steric hindrance and precluding further binding of HIV-specific IgGs. Alternatively, this may indicate competition between CD32 and gp120 for the binding of the same IgG.

We also studied the capacity of ex vivo infected $CD4^+$ T cells expressing CD32 to form ADCC-induced conjugates with NK cells. We observed a significantly higher frequency of T_{CD32}^{dim} – NK

doublets compared to T_{CD32}^{neg} cells (**Figure 4D**). This could be explained by the inefficient elimination of T_{CD32}^{dim} cells by ADCC (as shown in **Figure 1H**), more likely as a consequence of suboptimal antibody-induced immune synapse. This phenomenon has been previously described in HIV-infected macrophages where increased effector-target cell contact time was associated with relative resistance to cytotoxic T lymphocytes [49]. Indeed, when we tested the capacity of FACS-sorted and gp120-coated T_{CD32}^{dim} cells to activate NK cells, we observed that these cells triggered a less potent NK degranulation than their negative counterparts (**Figure 4E**), while IFN-γ was equally induced in both cases (**Figure S5C**). Overall, our results suggest that potential immune factors present in the plasma that are ligands of CD32 might promote a steric interference that precludes the subsequent binding of HIV-specific antibodies, leading to poor NK activation and therefore resistance to ADCC (as illustrated in **Figure 4F**).

HIV-infected cells expressing CD32 show higher proliferation potential after immune complexes engagement

We next explored the possibility that the engagement of IC to the CD32 molecule might induce cell proliferation, and therefore, contribute to their persistence. To study that, we performed ex vivo infection experiments and measured cell proliferation after IC engagement by flow cytometry. First, we observed that HIV-infected cells, and in particular infected cells expressing $CD32^{dim}$, had higher proliferative potential measured by the expression of Ki67 (median of 6.67% vs. 4.62% for T_{CD32}^{dim} and T_{CD32}^{neg}, respectively) (**Figure 5A and B**). Importantly, we observed that the addition of plasma from an HIV-infected patient (containing a high titer of Igs), induced significant proliferation of infected T_{CD32}^{dim} cells (median of 7.52% vs. 12.80% for basal condition and plasma HIV^{+}, respectively), which was abrogated when Fc receptor blockers were added to the culture (**Figure 5C**). Of note, no effect was observed after the addition of plasma from an HIV-negative donor (**Figure 5C**). In contrast, cell proliferation was unchanged in the infected T_{CD32}^{neg} population (**Figure 5D**). Overall, these results suggest that IC present in the plasma of PLWH could contribute to the perpetuation of the T_{CD32}^{dim} HIV-infected subset by inducing cell proliferation, besides protecting them from ADCC.

Effect of IL-15, IFN-α and anti-HLA-E antibody at enhancing the killing of HIV-infected T_{CD32}^{dim} cells

Given the unique properties of T_{CD32}^{dim} cells, we further explored several strategies to potentiate its elimination by NK cells. First, we tried to directly reinvigorate NK cells from HIV-infected PLWH (#52-58, **Table S1**) culturing them with the cytokines IL-15 or IFN-α. As expected and previously reported [50], we observed an enhanced performance of NK cells against the total gp120-coated $CD4^+$ T cell population when treated with IL-15, and to a lesser extent with IFN-α. However, neither IL-15 nor IFN-α was able to enhance the ADCC response against T_{CD32}^{dim} infected cells (**Figure 6A**). Moreover, we showed before that T_{CD32}^{dim} cells express a remarkable higher levels of the NK-ligand HLA-E. Thus, using ex vivo infected cells, we performed functional assays blocking the interaction of HLA-E with its cognate receptors on NK cells by adding specific antibodies against HLA-E (participants #38, 44, and 46-51, **Table S1**). In general, the NC response was not enhanced after HLA-E blocking, either in the whole population of infected cells ($p24^+$) (**Figure 6B**) or in the T_{CD32}^{dim} subpopulation (**Figure 6C**). However, we observed a more potent ADCC immune response against all infected cells after blocking HLA-E (**Figure 6D**), including the infected T_{CD32}^{dim} pool (**Figure 6E**). Remarkably, the use of an isotype control antibody also significantly enhanced the killing of all infected cells (**Figure 6D and E**), evidencing the non-specificity of the anti-HLA-E antibody at enhancing ADCC. Thus, blocking the interaction of HLA-E with its receptors in NK cells did not specifically reverse the intrinsic immune resistance of T_{CD32}^{dim} cells.

DISCUSSION

The presence of cellular and anatomical viral reservoirs, not susceptible to ART or antiviral immune responses, is the main barrier to cure the HIV infection. Thus, elucidating how these reservoirs are maintained for prolonged periods of time represents an important step towards the cure of HIV. Remarkably, we postulate a pivotal role of ADCC-NK in shaping the HIV reservoir during ART, being a novel route to avoid NK cell effector immunity by HIV-reservoir cells. We found that the expression of the molecule CD32 on productively HIV-infected cells is associated with a reduced susceptibility to ADCC activity by NK cells. Furthermore, when infected ex vivo, these cells express higher levels of the molecule HLA-E, which also limits NK-mediated killing. Last, upon interaction with immune complexes, their capacity to bind to HIV-specific antibodies decreases, while gaining the potential to proliferate. Considering that a significant proportion of HIV-latently infected cells expressed CD32 upon viral reactivation, as shown here and reported before [40], these cells will

indeed benefit from these described NK immune evasion mechanisms. Altogether, these factors may greatly contribute to perpetuating the persistence of the cell reservoir.

One of the main obstacles in the HIV cure field has been the lack of reliable markers to uniquely identify persistently infected cells. Amongst proposed molecules, we find immune checkpoint inhibitors such as PD-1 [51], the B cell surface marker CD20 [19], CD30 [20], or, more recently, a combination of several receptors [8]. However, the Fcγ receptor CD32 is perhaps one of the most promising HIV reservoir markers, since it is expressed during latent [9, 12] and transcriptionally-active infection [13, 15, 16, 52]; it has been localized in main tissue reservoirs such as the cervical tissue [6], lymph nodes [13, 16] and the gastrointestinal tract [15] and, in some cases, it has been associated with a very prominent enrichment for HIV DNA [6, 9, 12]. This molecule is typically expressed on myeloid cells or platelets, in which its function has been extensively studied [47]. While CD32 expressed on $CD4^+$ T cells is fully functional [36, 53], many questions remain unknown regarding the expression dynamics and function, in particular during HIV pathogenesis. In a recent study with SIV-infected non-human primates, $CD32^+CD4^+$ T cells were strongly increased in LNs, spleen, and intestine during SIV mac infection, were enriched in markers often expressed on HIV infected cells, and contained higher levels of actively transcribed SIV RNA [52]. Consistent with previous reports [13, 37], we detected dim levels of CD32 on $CD4^+$ T cells which increased upon ex vivo HIV infection or reactivation. This result is in line with a recent publication showing the ability of cells expressing CD32 to reactivate latent HIV [12]. Moreover, tissue-resident $CD4^+$ T cells with expression of CD32 have been reported in cervical samples in the absence of infection. Importantly, this fraction of cells was intrinsically enriched for the expression of molecules related to HIV susceptibility and long-term maintenance [6]. In this sense, cell proliferation is one of the most important mechanisms of cell reservoir maintenance in long-term ART-suppressed PLWH [3, 54, 55]. Importantly, we show that CD32-expressing cells had a higher proliferative potential in response to IC. Inherent proliferative capacity of this subset has recently been reported in a study demonstrating $CD4^+$ T cell activation upon CD32 ligation with antibodies or aggregated IgG [36]. Thus, understanding the mechanisms by which HIV-infected cells expressing CD32 are maintained in the human body could significantly advance the search for an HIV cure.

NK cells are key players in the defense against many pathogens, including HIV, being not only one of the first lines of protection but also essential modulators of the adaptive immune responses. Therefore, the acquisition of resistance mechanisms to any of the NK effector functions may

contribute to pathogen survival and, in the case of HIV, favor conditions for viral persistence. In this sense, it has been reported that NK cell immune pressure leads to viral sequence evolution [56], and HLA-mediated immune resistance mechanisms have been previously identified in productively HIV-infected cells [57, 58]. Moreover, resistance of reservoir cells to HIV-specific cytotoxic T cells has also been reported [59, 60], suggesting that viral persistence might be facilitated not only by cell proliferation mechanisms in the absence of viral antigen expression, but also by avoiding immune-mediated killing. NK cells recognize IgG–viral protein complexes, namely immune complexes, on infected cells via FcγRs to mediate ADCC, which is a potent mechanism to eliminate virally infected cells [61]. However, HIV has developed several strategies to evade this immune response. For instance, Vpu reduces the presence of viral antigens susceptible to recognition by antibodies on the surface of infected cells [62]. This accessory protein is responsible for the decreased expression of tetherin, a cellular host restriction factor that retains HIV virions on the cell surface, and therefore diminishes ADCC responses [62]. Moreover, Vpu and Nef downregulate CD4 expression on infected cells, preventing its interaction with Env trimers, which subsequently impedes the binding of ADCC-antibodies [63]. Overall, a proper antibody-induced immune synapse with NK cells is required to elicit a potent ADCC immune response, which depends on many factors, such as spatial configuration, valence of the antibody-epitope binding, antibody conformation, and the resulting size of the immune complex [64]. In our study, we show that the interaction of T_{CD32}^{dim} cells with IC present in plasma lead to suboptimal binding of HIV-specific antibodies, limiting ADCC. These results suggest that potential Igs, and likely other immune mediators such as pentraxins [48], might contribute to maintaining HIV-reservoir cells through the interaction with the CD32 receptor, conferring a diminished susceptibility to ADCC activity, which intrinsically requires the presence of immune complexes. This is not the first non-desirable effect of Igs identified in the context of an infectious disease; an antibody-dependent enhancement of infection has been extensively reported for Dengue infection [65]. The intrinsic nature of antibodies, with an antigen-binding fragment (Fab) and a crystallizable fragment (Fc) as separate functional domains, adds complexity to the multiple functions and interactions that ultimately contribute to modulate immunity [66]. Importantly, increased knowledge on the Fc effector functions of IgG antibodies is greatly contributing to the design of new therapeutic strategies based on Fc-optimized monoclonal antibodies to promote effective Fc effector activities [67]. In fact, a major line of research in the field currently focuses on the use of broadly neutralizing antibodies (bNAbs) as a therapeutic or prophylactic treatment for HIV infection, relying on the efficient blocking of the virus and the triggering of potent immune

354 effector responses, for example, through FcγR interactions [68, 69]. The potentiation of the NK
355 activity with these new approximations may help to overcome the intrinsic resistance of infected
356 cells expressing the CD32 receptor.

357 Furthermore, as previously reported by others, HIV infection maintains or even increases the
358 expression of the non-classical HLA-E molecule, which may contribute to the inhibition of the NK
359 cytotoxic response [44, 70]. Interestingly, we found enrichment of HLA-E expression in the pool of
360 HIV-infected cells expressing CD32, which could tilt the balance towards NK inhibition, therefore,
361 conferring an additional advantage to survive. HLA-E can interact with NK cells through two
362 receptors: NKG2A (inhibitory) and NKG2C (activating) [71]. Of note, the affinity of the NKG2A protein
363 for HLA-E is higher than that of NKG2C [72]. Further, $NKG2A^{+}$ NK cells do not typically express
364 NKG2C, thus representing a pool of NK cells that can potentially be restricted by HLA-E [73]. The
365 effect of HLA-E suppressing immune responses has been shown in several settings, including in the
366 context of senescence or tumors, where blocking its interaction reinvigorated effector functions [24,
367 25]. In addition, HLA-E has been shown to impair ADCC against HIV-expressing cells, while impeding
368 its interaction with NK cells improved the elimination of target cells [44]. Our results showed an
369 enhancement of NK-mediated killing of $CD32^{dim}$ HIV-infected cells by ADCC when HLA-E was blocked.
370 However, this potentiation was not specific, since the isotype control induced a similar effect. The
371 killing of aberrant cells mediated by NKs is determined by a complex balance of signaling received
372 through their multiple receptors which interact with molecules on the surface of undesired cells
373 [22]. Thus, other molecules expressed by T_{CD32}^{dim} cells may be contributing to elevating the threshold
374 for NK activation needed to eliminate this cell subpopulation in these individuals.

375 In recent years, major efforts have focused on the identification of compounds to reactivate
376 persistent HIV from its dormant state, with the ultimate goal to eliminate viral infection However,
377 it has become clear that the stimulation of the immune system is also a mandatory step for the
378 elimination of persistent HIV [74]. These approaches, known as *shock and kill*, have shown little
379 efficacy in several clinical trials in terms of HIV reservoir reactivation and the reduction of its size
380 [75]. This failure has been attributed to both, a poor capacity of the different LRAs to reactivate all
381 latent HIV [40], together with the dysfunction of the immune cells to kill viral reactivated cells [76].
382 Our results show that the magnitude of the killing also depended on the potency of the NK cells,
383 where NK cells from ART-suppressed PLWH with higher total HIV reservoir size were functionally
384 impaired. These results are in agreement with previous reports showing that HIV chronic infection

385 has a deleterious effect on NK cell function, which is not completely restored despite ART [26, 27].
386 To reinvigorate NK function in these subjects we treated NK cells with the cytokines IL-15 or IFN-α.
387 Despite a clear immune effect on the total infected population, we did not increase the killing of
388 T_{CD32}^{dim} cells. A plausible explanation would be the upregulation of NKG2A on NK cells mediated by
389 these cytokines [77, 78], which would further limit the killing of cells already expressing high levels
390 of HLA-E, such as T_{CD32}^{dim} cells.

391 A potential limitation of our study is the decline of HIV-specific antibody levels in ART-treated
392 PLWH [41, 79]. Despite this decline, functional ADCC activity mediated by NK cells remains
393 detectable in long-term virally-suppressed individuals [41]. Of relevance, we show here the
394 existence of functional ADCC activity using plasma samples from virologically-suppressed PLWH.
395 These antibodies induced significant NK-mediated elimination of the total pool of reactivated
396 latently infected cells in many samples, although the subpopulation expressing CD32 was more
397 resistant. Thus, our results suggest that, after viral reactivation, levels of HIV antigen expression
398 susceptible to recognition by immune cells such as NK may be induced. Also, that ADCC could play
399 a significant role in HIV persistence, highlighting the need for new strategies directed to impact
400 resistant reservoir cells such as T_{CD32}^{dim} cells. However, the limited number of these cells observed
401 in vivo in ART-treated PLWH restrains their study. In this sense, the few viral-reactivated cells
402 detected after LRA treatment from the natural latent reservoir impede an extensive assessment of
403 infected cells expressing CD32. Further, it is unclear which is the dynamic of CD32 expression on
404 individual cells after viral reactivation and if changes on its expression would affect ADCC activity.
405 Last, it is possible that infected T_{CD32}^{dim} cells are susceptible to cytotoxic $CD8^+$ T lymphocytes. Further
406 research on these aspects are warranted. However, based on our results, we may speculate that
407 this sort of immune resilient infected cells in vivo could certainly contribute to the source of viral
408 rebound when ART is interrupted, or they could initiate a low level of viral replication in tissues
409 where drugs are not able to fully penetrate. Moreover, their proliferative capacity in response to IC
410 situates these cells as candidates for cells supporting cellular proliferation, one of the main
411 mechanisms that perpetuate HIV reservoirs in vivo [80, 81].

412

413

414

Materials and Methods

Ethics statement and patient samples

PBMCs from PLWH were obtained from the HIV unit of the Hospital Universitari Vall d'Hebron in Barcelona, Spain. Study protocols were approved by the corresponding Ethical Committees (Institutional Review Board numbers PR(AG)270/2015 and PR(AG)39/2016). PBMCs from healthy donors were obtained from the Blood and Tissue Bank, Barcelona, Spain. All subjects recruited to this study were adults who provided written informed consent. Samples were completely anonymous and untraceable and were prospectively collected and cryopreserved in the Biobank (register number C.0003590). Information on plasma viral loads, $CD4^+$T cell counts, and time on ART from suppressed PLWH is summarized in **Table S1**.

Cells, virus, and reagents

PBMCs were obtained from PLWH and uninfected donors by Ficoll-Paque density gradient centrifugation and cryopreserved in liquid nitrogen. PBMCs were cultured in RPMI medium (Gibco) supplemented with 10% Fetal Bovine Serum (Gibco), 100 µg/ml streptomycin (Fisher Scientific), and 100 U/ml penicillin (Fisher Scientific) (R10 medium), and maintained at 37ºC in a 5% CO_2 incubator. For RNA FISH-flow assays, fresh PBMCs were obtained from a whole blood donation (400ml) from PLWH by Ficoll-Paque density gradient centrifugation and $CD4^+$ T cells were immediately isolated and used without previous cryopreservation.

All plasmids needed for the generation of viral stocks and delta molecular clones were obtained through the NIH AIDS Reagent Program. Viral stocks were generated by transfection of 293T cells with the plasmids encoding the different molecular clones, and the resulting viral particles were titrated in TZMbl cells using an enzyme luminescence assay (britelite plus kit; PerkinElmer) as described previously [82]. BaL gp120 recombinant protein was obtained through the NIH AIDS Reagent Program. The A32 antibody was obtained through the AIDS Research and Reference Program, NIAID, NIH (Cat#11438) from Dr. James E. Robinson [83]. Interleukin-2 (IL-2) was obtained from the Vall d´Hebron Hospital pharmacy. The pan-caspase inhibitor named Q-VD-OPh (quinolyl-valyl-O-methylaspartyl-[-2,6-difluorophenoxy]-methyl ketone was purchased from Selleckchem.

ADCC assay in cells coated with recombinant gp120

PBMCs from ART-suppressed PLWH, elite controllers, or uninfected donors were thawed and rested overnight in R10 medium. To exclude monocytes, PBMCs were cultured in a lying flask and adherent cells were discarded the next day. $CD4^+$ T cells and NK cells were isolated from cryopreserved PBMCs using commercial kits (MagniSort Human $CD4^+$ T Cell Enrichment; Affymetrix, and MagniSort™ Human NK cell Enrichment; eBioscience). Two rounds of cell separation were performed to maximize the purity of the cells (overall purity >85%). $CD4^+$ T cells were stained with the membrane lipid marker PKH67 (Sigma-Aldrich) following the manufacturer's instructions, for the stable identification of these target cells, and then coated with 1 µg of recombinant gp120 protein for 1h at RT. A pool of uncoated cells was used as a negative control. After coating, target cells were extensively washed in ice-cold R10 medium and dispensed in U-bottom 96-well plates (100,000 cells per well, 10 wells per condition). After that, $CD4^+$ T cells were incubated for 15 mins with plasma (1:1,000 dilution) from a viremic (high viral load in blood) HIV^+ patient. Then, NK effector cells were added at 1:1 target/effector ratio. Plates were centrifuged at 400xg for 3 mins and incubated for 4h at 37ºC and 5% CO_2. After incubation, cells were collected in FACs tubes, washed with staining buffer (PBS 3% FBS), and stained with anti-CCR7-PE-CF594 (150503, Becton Dickinson) for 30 mins at 37ºC. Next, cells were washed and stained with anti-CD3-AF700 (SK7, Biolegend), anti-CD45RO-BV605 (UCHL1, Biolegend), anti-CD32-PE-Cy7 (FUN-2, Biolegend), anti-HLA-DR-BV711 (L243, Biolegend), anti-CD20-BV786 (2H7, Biolegend), and anti-CD95-PE-Cy5 (DX2, Becton Dickinson) for 20 mins at RT. Finally, cells were washed with staining buffer (PBS 3% FBS) and fixed with PFA (2%). Flow cytometry particles for absolute cell counting ($5*10^4$/ml) (AccuCount Blank 5.0-5.9 µm, Cytognos) were added. Samples were acquired on an LSR Fortessa flow cytometer (Becton Dickinson) and analyzed using FlowJo V10 software. We calculated the % of killing as the number of cells that disappeared in each population, following the next formula:

$$\%\ \mathrm{ADCC} = 100 - \frac{Cells\ (gp120)}{Cells\ (no\ gp120)} * 100$$

Control cells non-coated with gp120 (no gp120 condition) but incubated with plasma allowed us to properly measure ADCC responses and rule out a possible non-specific activation of the NK cells mediated by the plasma.

In some experiments, we assessed the capacity of NK cells to perform ADCC after being stimulated with IFN-α or IL-15 (Miltenyi Biotec). In such cases, PBMCs were stimulated overnight with 5,000 U/ml IFN-α or 25 ng/ml of IL-15, and NK cells were isolated the next day.

Assessment of the gp120-coating in the different $CD4^+$ T cell subsets

$CD4^+$ T cells were coated with recombinant gp120 as described above and then stained with anti-CCR7-PE-CF594 (150503, Becton Dickinson), anti-CD3-AF700 (SK7, Biolegend), anti-CD45RO-BV605 (UCHL1, Biolegend), anti-CD32-PE-Cy7 (FUN-2, Biolegend), anti-HLA-DR-BV711 (L243, Biolegend), anti-CD20-BV786 (2H7, Biolegend) and anti-CD95-PE-Cy5 (DX2, Becton Dickinson) antibodies. Next, cells were incubated for 20 mins at RT with 5 µg/ml of A32 antibody (which binds to gp120 HIV protein). Then, cells were stained for 20 mins at RT with an anti-human FITC-labelled secondary antibody (dilution 1:100) (Thermo Fisher) for A32 detection. Samples were acquired on an LSR Fortessa flow cytometer and data analyzed using FlowJo.

Binding assessment of HIV-specific antibodies to T_{CD32}^{dim} cells

Isolated $CD4^+$ T cells from uninfected donors were coated with gp120 recombinant protein. To detect if IC might result in steric hindrance precluding the binding of HIV-specific Igs to the T_{CD32}^{dim} subset, we labeled the gp120-specific antibody (A32 mAb) with Allophycocyanin (APC) following the manufacturer instructions (Zenon Human IgG labeling kit, Invitrogen) and measured cell binding by flow cytometry. A pool of non-coated cells was used as a negative control. Cells were incubated with plasma containing high titer of non-HIV specific immune complexes (dilution 1,000) for 20 mins at RT. After, cells were incubated with A32-APC (3.3 µg/ml) for 25 minutes and labeled with anti-CD3-AF700 (SK7, Biolegend) and anti-CD32-PE-Cy7 (FUN-2, Biolegend). After, cells were washed once with PBS and stained with LIVE/DEAD Fixable Violet Viability (Invitrogen) for 20 mins at RT. Finally, cells were washed with PBS and fixed with PFA (2%). Samples were acquired on an LSR Fortessa flow cytometer and data analyzed using FlowJo.

ADCC-mediated NK cell activation of isolated T_{CD32}^{dim} cells.

For cell sorting experiments, 100 million PBMCs from healthy donors were stained with LIVE/DEAD violet viability (Invitrogen) for 20 mins at RT. After washing, cells were surface stained with anti-CD3-PerCP (SK7; Becton Dickinson), anti-CD56-FITC (B159, Becton Dickinson), anti-CD32-PE-Cy7 (FUN-2, Biolegend) and, anti-CD4-BV605 (RPA-T4, Becton Dickinson) antibodies for 20 mins at RT. Cells were then washed and immediately sorted using a BD FACSAria Cell Sorter. We sorted the populations $CD4^-CD3^-CD56^+$ (NK cells), $CD3^+CD4^+CD32^+$ (T_{CD32}^{dim}) and $CD3^+CD4^+CD32^-$ (T_{CD32}^-). Then, we performed the ADCC assay and measured NK cell activation by flow cytometry. Purity of the cells was >97% in all cases.

Sorted T_{CD32}^{dim} and T_{CD32}^{-} cells were coated with recombinant gp120 as described above and incubated with plasma from a viremic HIV-infected patient at 1:1,000 dilution 15 minutes before the addition of NK cells (ratio 1:2). Co-cultures were maintained for 4 h in a 96-well plate at 37ºC and 5% CO_2. NK cytotoxicity was assessed by measurement of CD107a and IFN-ɣ. As a positive control, we included NK cells cultured with 10 ng/ml PMA plus 1 µM ionomycin, and as a negative control, NK cells were cultured without any stimulus. CD107a-PE-Cy5 (H4A3; Beckton Dickinson), BD GolgiPlug Protein Transport Inhibitor (Becton Dickinson) and, BD GolgiStop Protein Transport Inhibitor containing monensin (Becton Dickinson) were also added to each well at the recommended concentrations at the beginning of cell culture. After incubation, cells were washed and stained with a viability dye (LIVE/DEAD Fixable Violet dead cell stain; Invitrogen). Cells were then stained with anti-CD56-FITC (B159; Becton Dickinson), anti-CD32-PE-Cy7 (FUN-2, Biolegend) and, anti-CD4-BV605 (RPA-T4, Becton Dickinson) antibodies for 20 mins at RT. After that, cells were washed and fixed and permeabilized with Fixation/Permeabilization Solution (Becton Dickinson) for 20 mins at 4ºC, washed with BD Perm/Wash buffer, and stained with anti-IFN-ɣ AF700 (Life technologies) for 30 mins at 4ºC. After washing, cells were fixed with PFA (2%) and acquired on an LSR Fortessa flow cytometer (Becton Dickinson). Flow cytometry particles for absolute cell counting ($5*10^4$/ml) (AccuCount Blank 5.0-5.9 µm, Cytognos) were added. Data were analyzed using FlowJo V10 software.

Ex vivo infection of unstimulated PBMCs

PBMCs from ART-suppressed PLWH or healthy donors were thawed and incubated overnight in R10 medium containing 40 U/ml IL-2. The next day, $CD4^+$ T cells were isolated using a commercial kit (MagniSort Human $CD4^+$ T Cell Enrichment; Affymetrix) and infected by incubation for 4 h at 37°C with 156,250 or 2,500 $TCID_{50}$ (50% tissue culture infectious dose) of $HIV_{NL4.3}$ or HIV_{BaL} viral strains, respectively. In some experiments, cells were infected by spinoculation at 1200**g* for 2 h at 37 ºC ($TCID_{50}$ of 78,125 and 625 for $HIV_{NL4.3}$ and HIV_{BaL}). Cells were then washed twice with PBS and cultured at 1 M/ml in a 96-well plate round-bottom with R10 containing 100 U/ml of IL-2 for the next 5 days. The resulting HIV-infected $CD4^+$ T cells were used for different experiments listed below.

Phenotyping of HIV-infected $CD4^+$ T cells

HIV-infected cells were stained with LIVE/DEAD AQUA viability (Invitrogen) for 30 mins at RT. After washing once with staining buffer, cells were stained with anti-ULBP1-PerCP (170818, R&D

Systems), anti-CD32-PE-Cy7 (FUN-2, Biolegend), anti-CD3-PE-Cy5 (UCHT-1, Biolegend), anti-CD4-AF700 (RPA-T4, Becton Dickinson), anti-HLA-E-APC (3D12, Biolegend), anti-CD155-BV786 (TX24, Becton Dickinson) and anti-MIC A/B –BV605 (6D4, Becton Dickinson) antibodies for 20 mins at RT. Cells were then fixed and permeabilized with Fixation/Permeabilization Solution (Becton Dickinson) for 20 mins at 4 ºC, washed with BD Perm/Wash buffer, and stained with anti-p24-PE (Beckman Coulter) for 20 mins on ice and 20 mins at RT. After washing with BD Perm/Wash buffer, cells were fixed with PFA (2%). Samples were acquired on an LSR Fortessa flow cytometer and data analyzed using FlowJo V10 software. Gating was performed according to the different FMO controls.

Assessment of the proliferative potential of T_{CD32}^{dim} cells

HIV-infected cells were incubated with plasma from a viremic HIV^+ patient or plasma from an uninfected healthy donor (dilution 1:1,000) for 4h at 37ºC and 5% CO_2. Additionally, a pool of HIV-infected cells previously treated with an Fc receptor blocker (human Fc block, Becton Dickinson) was used as a control. After incubation, cells were washed and stained with LIVE/DEAD Fixable Violet Viability (Invitrogen) for 20 mins at RT. Next, cells were washed with staining buffer and stained with anti-CCR7-PE-CF594 (150503, Becton Dickinson) for 30 mins at 37 ºC. After washing, cells were stained with anti-CD56-FITC (B159, Becton Dickinson), anti-CD3-AF700 (SK7, Biolegend), anti-CD45RO-BV605 (UCHL1, Biolegend), anti-CD32-PE-Cy7 (FUN-2, Biolegend), anti-CD20-BV786 (2H7, Biolegend), anti-CD95-PE-Cy5 (DX2, Becton Dickinson), and anti-CD4-APC (OKT4, Biolegend) for 20 mins at RT. Cells were then fixed and permeabilized with Fixation/Permeabilization Solution (Becton Dickinson) for 20 mins at 4ºC, washed with BD Perm/Wash buffer and stained with anti-p24-PE (KC57, Beckman Coulter) for 20 mins on ice and, during the additional 30 mins at RT an anti-Ki67-BV510 (B56, Becton Dickinson) was added. Finally, cells were washed and fixed with PFA (2%). Positive cells for the ki67 marker were determined according to FMO controls. Samples were acquired in an LSR Fortessa flow cytometer (Becton Dickinson) and analyzed with FlowJo V10 software.

Natural cytotoxicity and ADCC NK-based assays

5 days after infection, HIV-infected cells were placed in a 96 round bottom well plate at 100,000 cells/well (ten replicates). Autologous NK cells, previously isolated by negative selection using magnetic beads (MagniSort™ Human NK cell Enrichment Kit, eBioscience), from PBMCs thawed the day before the co-culture, were added at 1:1 ratio. For the study of the ADCC response, plasma from

a viremic HIV-infected patient containing a mix of antibodies targeting different HIV epitopes was added at 1:1,000 dilution to HIV-infected cells 15 minutes before the addition of NK cells. After, the plate was centrifuged at 400*g for 3 minutes to facilitate cell contact and then incubated at 37 ºC with 5% CO_2 for 4 h. After, cells were collected in FACs tubes, washed with PBS, and stained with LIVE/DEAD Fixable Violet Viability (Invitrogen) for 20 mins at RT. Next, cells were washed with staining buffer and stained first with anti-CCR7-PE-CF594 for 30 mins at 37 ºC, and after an additional wash, with anti-CD56-FITC (B159, Becton Dickinson), anti-CD3-AF700 (SK7, Biolegend), anti-CD45RO-BV605 (UCHL1, Biolegend), anti-CD32-PE-Cy7 (FUN-2, Biolegend), anti-CD20-BV786 (2H7, Biolegend), anti-CD95-PE-Cy5 (DX2, Becton Dickinson), and anti-CD4-APC (OKT4, Biolegend) antibodies for 20 mins at RT. Cells were then fixed and permeabilized with Fixation/Permeabilization Solution (Becton Dickinson) for 20 mins at 4ºC, washed with BD Perm/Wash buffer, and stained with anti-p24-PE (KC57, Beckman Coulter) for 20 mins on ice and 20 mins at RT. Finally, cells were washed and fixed with PFA (2%). Flow cytometry particles for absolute cell counting ($5*10^4$/ml) (AccuCount Blank 5.0-5.9 µm, Cytognos) were added. We also included a non-infected condition. Gating of the CD32 subpopulation was done according to FMO controls. Samples were acquired in an LSR Fortessa flow cytometer and analyzed with FlowJo software. The percentage of ADCC killing was determined by calculating the number of cells that disappeared in each infected population, normalizing numbers to the condition of HIV-infected $CD4^+$ T cells plus NK cells (in the absence of plasma). The NC response was quantified as the reduction in the % of p24 HIV protein in T_{CD32}^{neg} and T_{CD32}^{dim} subsets, in comparison to the % of p24 in these subsets in basal conditions in the absence of NK cells. In the experiments assessing the effect of blocking HLA-E, HIV-infected cells were previously incubated with 10 µg/ml of anti-human HLA-E (clone 3D12, Biolegend) antibody for 20 mins at RT, or with an isotype control mouse IgG1 (Becton Dickinson). In these assays, cells were first stained with AQUA viability (Thermo Fisher), then with a panel of surface antibodies: anti-ULBP1-PerCP (170818, R&D Systems), anti-CD56-FITC (B159, Beckton Dickinson), anti-CD32-PE-Cy7 (FUN-2, Biolegend), anti-CD3-PE-Cy5 (UCHT-1, Biolegend), anti-CD4-AF700 (RPA-T4, Becton Dickinson), anti-HLA-E-APC (3D12, Biolegend), anti-CD155-BV786 (TX24, Becton Dickinson), anti-MIC A/B –BV605 (6D4, Becton Dickinson); and finally intracellularly stained with anti-p24-PE (KC57, Beckman Coulter) as previously described.

Cell conjugates were identified by flow cytometry and quantified as follow: live lymphocytes (isolated $CD4^+$ T and NK cells) were gated after excluding contamination with B cells and monocytes. Then, HIV-infected cells were identified as $p24^+$ cells in $CD3^+$ cells, from which we selected separately

595 both, CD32^{dim} and CD32^{neg} cells. From CD32^{dim} and CD32^{neg} populations we gated cell doublets by
596 side scatter signals, and then we determined the fraction of cell doublets composed by CD4^{+} T cells
597 (CD3+ and CD32^{dim} or CD32^{neg}) and NK cells (identified as CD56^{+} cells).

598 **Detection of cells expressing HIV-1 RNA by the RNA FISH-flow assay**

599 PBMCs from nine ART-treated PLWH were obtained from a whole blood donation (400ml) and
600 CD4^{+} T cells were isolated by a negative selection kit (MagniSort Human CD4^{+} T Cell Enrichment;
601 eBioscience). At least 6x10^{6} of freshly-isolated CD4^{+} T cells were studied per condition, being
602 subjected to viral reactivation with different LRAs (Ingenol and Romidepsin), and including the
603 positive (PMA plus ionomycin) and negative controls (medium condition). Before viral reactivation,
604 cells were pre-incubated with the pan-caspase inhibitor Q-VD-OPh (Selleckchem) for 2h. In addition,
605 to prevent new rounds of viral infection during HIV reactivation, the cells were treated with LRAs in
606 the presence of Raltegravir (1uM) for 22h. Afterward, the RNA FISH-flow assay was performed
607 according to the manufacturer's instructions (Human PrimerFlow RNA Assay, eBioscience) with
608 some modifications as previously described [39]. Briefly, after antibody staining and cell fixation and
609 permeabilization, cells were ready for hybridization with a set of 50 probes spanning the whole Gag-
610 Pol HIV mRNA sequence (bases 1165 to 4402 of the HXB2 consensus genome). Next, the cells were
611 subjected to amplification signal steps, and HIV RNA was detected using Alexa Fluor 647-labeled
612 probes. In these experiments, for surface antigen labeling, anti-human CD3 (AF700, Biolegend), anti-
613 human CD32 (PE-Cy7, Biolegend), anti-human CD20 (BV785, Biolegend), and anti-human HLA-DR
614 (BV711, Biolegend) antibodies were used, and cell viability analyzed with violet viability dye
615 (Invitrogen). Samples were analyzed with the LSR Fortessa flow cytometer, and the results were
616 analyzed with FlowJo v10 software.

617 **Ex vivo viral reactivation of the natural reservoir from ART-suppressed PLWH.**

618 CD4^{+} T lymphocytes from ART-suppressed PLWH were isolated as described above and cultured
619 in R10 medium with Q-VD-OPh (Selleckchem) for 2h in the presence of Raltegravir (1 µM), Darunavir
620 (1 µM), and Nevirapine (1 µM) to prevent new rounds of viral infection. After 2h, PMA plus
621 ionomycin (PMA 81 nM; ionomycin 1 µM) were added to the cell culture as a latency reversal agent
622 and left for 18h to reactivate latent HIV. After viral reactivation, cells were subjected to cytotoxicity
623 and ADCC assays as previously described here. For these experiments, we used the autologous
624 plasma from each patient. After, cells were stained with LIVE/DEAD Far Red viability for 20 minutes

at RT and then with anti-CD32 (FITC, Biolegend) and anti-CD3 (PerCP, Becton Dickinson) antibodies for 20 minutes at RT. After the cell surface staining, cells were fixed and permeabilized with Fixation/Permeabilization Solution (Becton Dickinson) for 20 mins at 4ºC, washed with BD Perm/Wash buffer, and stained with anti-p24-PE (Beckman Coulter) for 20 mins on ice and 20 mins at RT. Finally, cells were washed and fixed with PFA (2%). Samples were acquired in a FACSCalibur flow cytometer (Becton Dickinson) and analyzed with FlowJo V10 software. The limit of detection of the assay was established at 50 $p24^+$ cells/million $CD4^+$ T cells (**Figure S3C**).

Quantification of HIV DNA and HIV RNA by quantitative PCR

$CD4^+$ T lymphocytes were enriched from total PBMCs using a negative selection kit (MagniSort Human $CD4^+$ T Cell Enrichment, eBioscience). Then, $CD4^+$ T cells were fractioned to extract RNA or quantify the HIV DNA from cell lysates. $CD4^+$ T cells for DNA analysis were immediately lysed with proteinase K-containing lysis buffer (at 55ºC overnight and 95ºC for 5 minutes). The HIV DNA in the cell lysates was quantified by qPCR using primers and probes specific for the 1-LTR HIV region (LTR forward 5'-TTAAGCCTCAATAAAGCTTGCC-3', LTR reverse 5'-GTTCGGGCGCCACTGCTAG-3' and probe 5' /56-FAM/CCAGAGTCA/ZEN/CACAACAGACGGGCA/31ABkFQ/ 3'). CCR5 gene was used for cell input normalization. Samples were analyzed in an Applied Biosystems 7000 Real-Time PCR System. For Viral RNA quantification, $CD4^+$ T cells were subjected to RNA extraction using the mirVana kit following the manufacturer's instructions (Ambion). Reverse transcription of RNA to cDNA was performed with SuperScriptIII (Invitrogen), and cDNA was quantified by qPCR with primers against the HIV long terminal repeat (LTR). Quantification of RNA and DNA copies was performed using a standard curve, and values were normalized to 1 million $CD4^+$ T cells.

Statistical analyses

Statistical analyses were performed with Prism software, version 6.0 (GraphPad). A P value <0.05 was considered significant.

Author contributions

M.B. designed, directed, and interpreted experiments. A.A-G and J.G-E designed and performed experiments, analyzed the data, and interpreted experiments. A.A-G, J.B, J.N, A.C, B.P, P.S, M.G, and V.F were responsible for recruitment, specimen handling and storage, and related clinical data

collection. A.A-G and M.B wrote the initial manuscript, and all of us contributed to the editing of the manuscript.

Acknowledgments

This study was supported by the Spanish Secretariat of Science and Innovation and FEDER funds (grants SAF2015-67334-R and RTI2018-101082-B-I00 [MINECO/FEDER]), the Spanish "Ministerio de Economia y Competitividad, Instituto de Salud Carlos III" (ISCIII, PI17/01470), GeSIDA and the Spanish AIDS network Red Temática Cooperativa de Investigación en SIDA (RD16/0025/0007), the Fundació La Marató TV3 (grants 201805-10FMTV3 and 201814-10FMTV3) and the Gilead fellowships GLD19/00084 and GLD18/00008. M.B is supported by the Miguel Servet program funded by the Spanish Health Institute Carlos III (CP17/00179). A.A-G is supported by the Spanish Secretariat of Science and Innovation Ph.D. fellowship (BES-2016-076382). The funders had no role in study design, data collection, and analysis, the decision to publish, or preparation of the manuscript.

Data Availability

The authors declare that the data supporting the findings of this study are available within the paper and its supplementary information files. Source data are provided with this paper.

REFERENCES

1. Klatt, N.R., et al., *Immune activation and HIV persistence: implications for curative approaches to HIV infection.* Immunol Rev, 2013. **254**(1): p. 326-42.
2. Joos, B., et al., *HIV rebounds from latently infected cells, rather than from continuing low-level replication.* Proc Natl Acad Sci U S A, 2008. **105**(43): p. 16725-30.
3. Chomont, N., et al., *HIV reservoir size and persistence are driven by T cell survival and homeostatic proliferation.* Nat Med, 2009. **15**(8): p. 893-900.
4. Grau-Exposito, J., et al., *A Novel Single-Cell FISH-Flow Assay Identifies Effector Memory CD4(+) T cells as a Major Niche for HIV-1 Transcription in HIV-Infected Patients.* mBio, 2017. **8**(4).
5. Buzon, M.J., et al., *HIV-1 persistence in CD4+ T cells with stem cell-like properties.* Nat Med, 2014. **20**(2): p. 139-42.
6. Cantero-Perez, J., et al., *Resident memory T cells are a cellular reservoir for HIV in the cervical mucosa.* Nat Commun, 2019. **10**(1): p. 4739.
7. Darcis, G., B. Berkhout, and A.O. Pasternak, *The Quest for Cellular Markers of HIV Reservoirs: Any Color You Like.* Front Immunol, 2019. **10**: p. 2251.

8. Neidleman, J., et al., *Phenotypic analysis of the unstimulated in vivo HIV CD4 T cell reservoir.* Elife, 2020. **9**.
9. Descours, B., et al., *CD32a is a marker of a CD4 T-cell HIV reservoir harbouring replication-competent proviruses.* Nature, 2017. **543**(7646): p. 564-567.
10. Bertagnolli, L.N., et al., *The role of CD32 during HIV-1 infection.* Nature, 2018. **561**(7723): p. E17-E19.
11. Perez, L., et al., *Conflicting evidence for HIV enrichment in CD32(+) CD4 T cells.* Nature, 2018. **561**(7723): p. E9-E16.
12. Darcis, G., et al., *CD32(+)CD4(+) T Cells Are Highly Enriched for HIV DNA and Can Support Transcriptional Latency.* Cell Rep, 2020. **30**(7): p. 2284-2296 e3.
13. Abdel-Mohsen, M., et al., *CD32 is expressed on cells with transcriptionally active HIV but does not enrich for HIV DNA in resting T cells.* Sci Transl Med, 2018. **10**(437).
14. Badia, R., et al., *CD32 expression is associated to T-cell activation and is not a marker of the HIV-1 reservoir.* Nat Commun, 2018. **9**(1): p. 2739.
15. Vasquez, J.J., et al., *CD32-RNA Co-localizes with HIV-RNA in CD3+ Cells Found within Gut Tissues from Viremic and ART-Suppressed Individuals.* Pathog Immun, 2019. **4**(1): p. 147-160.
16. Noto, A., et al., *CD32(+) and PD-1(+) Lymph Node CD4 T Cells Support Persistent HIV-1 Transcription in Treated Aviremic Individuals.* J Virol, 2018. **92**(20).
17. Martin, G.E., et al., *CD32-Expressing CD4 T Cells Are Phenotypically Diverse and Can Contain Proviral HIV DNA.* Front Immunol, 2018. **9**: p. 928.
18. Gálvez, C., et al., *Atlas of the HIV-1 Reservoir in Peripheral CD4 T Cells of Individuals on Successful Antiretroviral Therapy.* 2021. **12**(6): p. e0307821.
19. Serra-Peinado, C., et al., *Expression of CD20 after viral reactivation renders HIV-reservoir cells susceptible to Rituximab.* Nat Commun, 2019. **10**(1): p. 3705.
20. Hogan, L.E., et al., *Increased HIV-1 transcriptional activity and infectious burden in peripheral blood and gut-associated CD4+ T cells expressing CD30.* PLoS Pathog, 2018. **14**(2): p. e1006856.
21. Vivier, E., et al., *Functions of natural killer cells.* Nat Immunol, 2008. **9**(5): p. 503-10.
22. Lanier, L.L., *Up on the tightrope: natural killer cell activation and inhibition.* Nat Immunol, 2008. **9**(5): p. 495-502.
23. Bottino, C., et al., *Cellular ligands of activating NK receptors.* Trends Immunol, 2005. **26**(4): p. 221-6.
24. Andre, P., et al., *Anti-NKG2A mAb Is a Checkpoint Inhibitor that Promotes Anti-tumor Immunity by Unleashing Both T and NK Cells.* Cell, 2018. **175**(7): p. 1731-1743 e13.
25. Pereira, B.I., et al., *Senescent cells evade immune clearance via HLA-E-mediated NK and CD8(+) T cell inhibition.* Nat Commun, 2019. **10**(1): p. 2387.
26. Nabatanzi, R., et al., *Aberrant natural killer (NK) cell activation and dysfunction among ART-treated HIV-infected adults in an African cohort.* Clin Immunol, 2019. **201**: p. 55-60.
27. Lichtfuss, G.F., et al., *Virologically suppressed HIV patients show activation of NK cells and persistent innate immune activation.* J Immunol, 2012. **189**(3): p. 1491-9.
28. Florez-Alvarez, L., J.C. Hernandez, and W. Zapata, *NK Cells in HIV-1 Infection: From Basic Science to Vaccine Strategies.* Front Immunol, 2018. **9**: p. 2290.
29. Marras, F., et al., *Control of the HIV-1 DNA Reservoir Is Associated In Vivo and In Vitro with NKp46/NKp30 (CD335 CD337) Inducibility and Interferon Gamma Production by Transcriptionally Unique NK Cells.* J Virol, 2017. **91**(23).

30. Olesen, R., et al., *Innate Immune Activity Correlates with CD4 T Cell-Associated HIV-1 DNA Decline during Latency-Reversing Treatment with Panobinostat.* J Virol, 2015. **89**(20): p. 10176-89.
31. Jost, S. and M. Altfeld, *Evasion from NK cell-mediated immune responses by HIV-1.* Microbes Infect, 2012. **14**(11): p. 904-15.
32. Alpert, M.D., et al., *ADCC develops over time during persistent infection with live-attenuated SIV and is associated with complete protection against SIV(mac)251 challenge.* PLoS Pathog, 2012. **8**(8): p. e1002890.
33. Pollara, J., et al., *High-throughput quantitative analysis of HIV-1 and SIV-specific ADCC-mediating antibody responses.* Cytometry A, 2011. **79**(8): p. 603-12.
34. Haynes, B.F., et al., *Immune-correlates analysis of an HIV-1 vaccine efficacy trial.* N Engl J Med, 2012. **366**(14): p. 1275-86.
35. Gomez-Roman, V.R., et al., *A simplified method for the rapid fluorometric assessment of antibody-dependent cell-mediated cytotoxicity.* J Immunol Methods, 2006. **308**(1-2): p. 53-67.
36. Holgado, M.P., et al., *CD32 Ligation Promotes the Activation of CD4(+) T Cells.* Front Immunol, 2018. **9**: p. 2814.
37. Garcia, M., et al., *CD32 Expression is not Associated to HIV-DNA content in CD4 cell subsets of individuals with Different Levels of HIV Control.* Sci Rep, 2018. **8**(1): p. 15541.
38. Mikulak, J., et al., *Natural killer cells in HIV-1 infection and therapy.* AIDS, 2017. **31**(17): p. 2317-2330.
39. Grau-Expósito J, S.-P.C., Miguel L, Navarro J, Curran A, Burgos J, Ocaña I, Ribera E, Torrella A, Planas B, Rosa Badía, Castellví J, Falcò V, Crespo M, Buzon MJ, *A Novel Single-Cell FISH-Flow Assay Identifies Effector Memory CD4 T cells as a Major Niche for HIV-1 Transcription in HIV-Infected Patients.* mBIO, 2017.
40. Grau-Exposito, J., et al., *Latency reversal agents affect differently the latent reservoir present in distinct CD4+ T subpopulations.* PLoS Pathog, 2019. **15**(8): p. e1007991.
41. Madhavi, V., et al., *Antibody-dependent effector functions against HIV decline in subjects receiving antiretroviral therapy.* J Infect Dis, 2015. **211**(4): p. 529-38.
42. Tremblay-McLean, A., et al., *Expression Profiles of Ligands for Activating Natural Killer Cell Receptors on HIV Infected and Uninfected CD4(+) T Cells.* Viruses, 2017. **9**(10).
43. Apps, R., et al., *HIV-1 Vpu Mediates HLA-C Downregulation.* Cell Host Microbe, 2016. **19**(5): p. 686-95.
44. Ward, J.P., M.I. Bonaparte, and E. Barker, *HLA-C and HLA-E reduce antibody-dependent natural killer cell-mediated cytotoxicity of HIV-infected primary T cell blasts.* AIDS, 2004. **18**(13): p. 1769-79.
45. Alevy, Y.G., J. Tucker, and T. Mohanakumar, *CD32A (Fc gamma RIIa) mRNA expression and regulation in blood monocytes and cell lines.* Mol Immunol, 1992. **29**(11): p. 1289-97.
46. Veri, M.C., et al., *Monoclonal antibodies capable of discriminating the human inhibitory Fcgamma-receptor IIB (CD32B) from the activating Fcgamma-receptor IIA (CD32A): biochemical, biological and functional characterization.* Immunology, 2007. **121**(3): p. 392-404.
47. Anania, J.C., et al., *The Human FcgammaRII (CD32) Family of Leukocyte FcR in Health and Disease.* Front Immunol, 2019. **10**: p. 464.
48. Lu, J., et al., *Structural recognition and functional activation of FcgammaR by innate pentraxins.* Nature, 2008. **456**(7224): p. 989-92.

49. Clayton, K.L., et al., *Resistance of HIV-infected macrophages to CD8(+) T lymphocyte-mediated killing drives activation of the immune system.* Nat Immunol, 2018. **19**(5): p. 475-486.
50. Garrido, C., et al., *Interleukin-15-Stimulated Natural Killer Cells Clear HIV-1-Infected Cells following Latency Reversal Ex Vivo.* J Virol, 2018. **92**(12).
51. Fromentin, R., et al., *CD4+ T Cells Expressing PD-1, TIGIT and LAG-3 Contribute to HIV Persistence during ART.* PLoS Pathog, 2016. **12**(7): p. e1005761.
52. Huot, N., et al., *CD32(+)CD4(+) T Cells Sharing B Cell Properties Increase With Simian Immunodeficiency Virus Replication in Lymphoid Tissues.* Front Immunol, 2021. **12**: p. 695148.
53. Engelhardt, W., J. Matzke, and R.E. Schmidt, *Activation-dependent expression of low affinity IgG receptors Fc gamma RII(CD32) and Fc gamma RIII(CD16) in subpopulations of human T lymphocytes.* Immunobiology, 1995. **192**(5): p. 297-320.
54. Gantner, P., et al., *Single-cell TCR sequencing reveals phenotypically diverse clonally expanded cells harboring inducible HIV proviruses during ART.* Nat Commun, 2020. **11**(1): p. 4089.
55. Simonetti, F.R., et al., *Clonally expanded CD4+ T cells can produce infectious HIV-1 in vivo.* Proc Natl Acad Sci U S A, 2016. **113**(7): p. 1883-8.
56. Alter, G., et al., *HIV-1 adaptation to NK-cell-mediated immune pressure.* Nature, 2011. **476**(7358): p. 96-100.
57. Cohen, G.B., et al., *The selective downregulation of class I major histocompatibility complex proteins by HIV-1 protects HIV-infected cells from NK cells.* Immunity, 1999. **10**(6): p. 661-71.
58. Bonaparte, M.I. and E. Barker, *Killing of human immunodeficiency virus-infected primary T-cell blasts by autologous natural killer cells is dependent on the ability of the virus to alter the expression of major histocompatibility complex class I molecules.* Blood, 2004. **104**(7): p. 2087-94.
59. Ren, Y., et al., *BCL-2 antagonism sensitizes cytotoxic T cell-resistant HIV reservoirs to elimination ex vivo.* J Clin Invest, 2020. **130**(5): p. 2542-2559.
60. Huang, S.H., et al., *Latent HIV reservoirs exhibit inherent resistance to elimination by CD8+ T cells.* J Clin Invest, 2018. **128**(2): p. 876-889.
61. Forthal, D.N. and A. Finzi, *Antibody-dependent cellular cytotoxicity in HIV infection.* AIDS (London, England), 2018. **32**(17): p. 2439-2451.
62. Arias, J.F., et al., *Tetherin antagonism by Vpu protects HIV-infected cells from antibody-dependent cell-mediated cytotoxicity.* Proc Natl Acad Sci U S A, 2014. **111**(17): p. 6425-30.
63. Veillette, M., et al., *Interaction with cellular CD4 exposes HIV-1 envelope epitopes targeted by antibody-dependent cell-mediated cytotoxicity.* J Virol, 2014. **88**(5): p. 2633-44.
64. Murin, C.D., *Considerations of Antibody Geometric Constraints on NK Cell Antibody Dependent Cellular Cytotoxicity.* Front Immunol, 2020. **11**: p. 1635.
65. Martina, B.E., P. Koraka, and A.D. Osterhaus, *Dengue virus pathogenesis: an integrated view.* Clin Microbiol Rev, 2009. **22**(4): p. 564-81.
66. Lu, L.L., et al., *Beyond binding: antibody effector functions in infectious diseases.* Nat Rev Immunol, 2018. **18**(1): p. 46-61.
67. Bournazos, S. and J.V. Ravetch, *Fcgamma Receptor Function and the Design of Vaccination Strategies.* Immunity, 2017. **47**(2): p. 224-233.
68. Hessell, A.J., et al., *Fc receptor but not complement binding is important in antibody protection against HIV.* Nature, 2007. **449**(7158): p. 101-4.

69. Bournazos, S., et al., *Broadly neutralizing anti-HIV-1 antibodies require Fc effector functions for in vivo activity.* Cell, 2014. **158**(6): p. 1243-1253.
70. Martini, F., et al., *HLA-E up-regulation induced by HIV infection may directly contribute to CD94-mediated impairment of NK cells.* Int J Immunopathol Pharmacol, 2005. **18**(2): p. 269-76.
71. Kanevskiy, L., et al., *Dimorphism of HLA-E and its Disease Association.* Int J Mol Sci, 2019. **20**(21).
72. Kaiser, B.K., et al., *Structural basis for NKG2A/CD94 recognition of HLA-E.* Proc Natl Acad Sci U S A, 2008. **105**(18): p. 6696-701.
73. Brostjan, C., et al., *Differential expression of inhibitory and activating CD94/NKG2 receptors on NK cell clones.* J Immunol Methods, 2002. **264**(1-2): p. 109-19.
74. Ward, A.R., T.M. Mota, and R.B. Jones, *Immunological approaches to HIV cure.* Semin Immunol, 2020: p. 101412.
75. Spivak, A.M. and V. Planelles, *Novel Latency Reversal Agents for HIV-1 Cure.* Annu Rev Med, 2018. **69**: p. 421-436.
76. Deng, K., et al., *Broad CTL response is required to clear latent HIV-1 due to dominance of escape mutations.* Nature, 2015. **517**(7534): p. 381-5.
77. Merino, A., et al., *Chronic stimulation drives human NK cell dysfunction and epigenetic reprograming.* J Clin Invest, 2019. **129**(9): p. 3770-3785.
78. Mori, S., et al., *Differential regulation of human NK cell-associated gene expression following activation by IL-2, IFN-alpha and PMA/ionomycin.* Int J Oncol, 1998. **12**(5): p. 1165-70.
79. Jensen, S.S., et al., *HIV-Specific Antibody-Dependent Cellular Cytotoxicity (ADCC) -Mediating Antibodies Decline while NK Cell Function Increases during Antiretroviral Therapy (ART).* PLoS One, 2015. **10**(12): p. e0145249.
80. Sengupta, S. and R.F. Siliciano, *Targeting the Latent Reservoir for HIV-1.* Immunity, 2018. **48**(5): p. 872-895.
81. Halvas, E.K., et al., *HIV-1 viremia not suppressible by antiretroviral therapy can originate from large T cell clones producing infectious virus.* J Clin Invest, 2020. **130**(11): p. 5847-5857.
82. Li, M., et al., *Genetic and neutralization properties of subtype C human immunodeficiency virus type 1 molecular env clones from acute and early heterosexually acquired infections in Southern Africa.* J Virol, 2006. **80**(23): p. 11776-90.
83. Moore, J.P., et al., *Immunochemical analysis of the gp120 surface glycoprotein of human immunodeficiency virus type 1: probing the structure of the C4 and V4 domains and the interaction of the C4 domain with the V3 loop.* J Virol, 1993. **67**(8): p. 4785-96.

Table S1. Clinical data of PLWH included in the study.

# Patient ID	Time since HIV diagnosis (months)	CD4 Cell Count (cells/µl)	%CD4	Viral Load (copies/ml)	Time on ART- VL-suppressed (months)	ART regimen
1 (EC)	287	1170	52.8	<50	-	UNT
2 (EC)	11	840	23.7	<50	-	UNT
3 (EC)	51	1030	36.0	<50	-	UNT
4 (EC)	104	1610	46.0	<50	-	UNT
5 (EC)	59	890	NA	<50	-	UNT
6 (EC)	321	490	20.4	<50	-	UNT
7 (EC)	189	410	23.2	<50	-	UNT
8	221	1240	40.1	<50	158	EFV+TDF+3TC
9	373	960	33.7	<50	113	COB+DRV
10	301	1050	27.0	<50	142	COB+DRV
11	102	1040	37.0	<50	61	DRV+RTV+3TC
12	128	760	28.1	<50	59	3TC+ABV+RPV
13	73	660	40.4	<50	67	3TC+ABV+NVP
14	333	670	24.1	<50	86	RPV+COB+DRV
15	67	830	28.6	<50	62	3TC+ABV+RPV
16	142	630	36.0	<50	85	FTC+RPV+TDF
17	213	1000	42.4	<50	76	FTC+RPV+TDF
18	107	600	31.0	<50	105	FTC+RPV+TDF
19	161	1150	36.5	<50	85	FTC+NVP+TDF
20	90	710	38.3	<50	85	FTC+TDF+COB+ATV
21	136	810	44.3	<50	90	3TC+ABV+EFV
22	86	1000	37.0	<50	66	FTC+RPV+TDF
23	319	689	24.5	<50	115	ETV+RTG+RTV+DRV
24	54	530	24.0	<50	51	RTG+3TC+ABV
25	119	750	27.9	<50	97	3TC+ABV+DTG
26	95	660	49.5	<50	69	ETV+FTC++TDF
27	323	2090	46.0	<50	43	3TC+ABV+DTG
28	240	NA	25.6	<50	71	TDF+COB+DRV
29	76	540	25.0	<50	56	RPV+FTC+TDF
30	65	570	26.2	<50	62	3TC+ABV+RTG
31	248	1050	32.0	<50	84	COB+DRV
32	293	560	24.4	<50	80	RTG+COB+DRV
33	113	600	38.7	<50	95	EFV+FTC+TDF
34	267	570	18.1	<50	98	RTG+FTC+TAF
35	134	870	48.7	<50	97	COB+DRV+DTG
36	98	680	54.0	<50	86	3TC+ABV+RPV
37	54	350	24.0	<50	48	RTV+FTC+TDF
38	121	850	35.6	<50	88	3TC+ABV+DTG
39	286	1060	30.3	<50	82	3TC+ABV+DTG
40	99	930	46.0	<50	79	RPV+FTC+TDF

41	94	1160	31.0	<50	73	3TC+ABV+DTG
42	73	310	13.3	<50	67	3TC+ABV+RPV
43	99	450	25.0	<50	96	3TC+ABV+RPV
44	89	690	35.2	<50	85	RPV+FTC+TDF
45	98	800	40.2	<50	89	FTC+RTV+TAF
46	63	660	29.8	<50	24	BIC+FTC+TAF
47	116	550	38.4	<50	92	FTC+RPV+TDF
48	169	1040	37.4	<50	101	3TC+ABV+NVP
49	146	860	37.4	<50	54	RPV+FTC+TDF
50	60	890	34.5	<50	55	3TC+ABV+DTG
51	40	570	27.4	<50	28	3TC+ABV+DTG
52	214	890	37.0	<50	99	EFV+FTC+TDF
53	135	790	27.5	<50	90	RPV+FTC+TDF
54	90	640	24.2	<50	62	DRV+FTC+TDF+RTV
55	193	890	34.1	<50	85	EFV+FTC+TDF
56	80	500	28.6	<50	72	RPV+FTC+TDF
57	178	850	39.5	<50	81	EFV+FTC+TDF
58	103	1170	44.0	<50	58	RPV+FTC+TDF
59	72	800	23.1	<50	18	ABV/3TC+DTG
60	33	490	21.0	<50	28	TDF/FTC+EVG/c
61	31	560	27.9	<50	11	TDF/FTC+EVG/c
62	49	1070	38.1	<50	39	TDF+FTC+EFV
63	31	810	34.7	<50	22	ABV/3TC+DTG
64	42	1150	37.0	<50	37	ABV/3TC+RPV
65	13	1760	57.7	<50	>13	TDF/FTC+EVG/c
66	55	970	NA	<50	45	ABV/3TC+DGT
67	168	540	NA	<50	54	TDF/FTC+EVG/c
68	38	920	39.8	<50	27	COB+FTC+TAF+EVG
69	83	730	34.2	<50	25	COB+FTC+TAF+EVG
70	44	360	31.0	<50	35	RTG+3TC+ABV
71	116	590	23.0	<50	96	RPV+FTC+TDF
72	72	930	44.8	50	60	3TC+DTG
73	106	580	28.3	<50	34	BIC+FTC+TAF
74	97	640	29.0	<50	63	FTC+RPV+TAF
75	96	540	35.0	50	74	RPV+FTC+TDF
76	121	810	38.4	<50	45	BIC+FTC+TAF
77	169	650	35.7	<50	92	3TC+ABV+DTG
78	163	600	29.3	<50	70	FTC+RPV+TDF
79	105	670	32.1	<50	103	FTC+RPV+TDF
80	156	700	48.5	<50	118	COB+DRV+DTG
81	62	1420	44.3	<50	54	3TC+DTG
82	319	280	27.0	<50	70	MRV+DRV+RTV+DTG
83	100	1080	37.4	<50	84	RPV+FTC+TDF
84	51	860	31.2	<50	33	3TC+ABV+DTG
85	156	1240	44.0	<50	35	BIC+FTC+TDF
86	158	990	48.9	<50	81	3TC+ABV+DTG

87	58	600	32.1	<50	56	DTG+3TC
88	448	1420	44.0	<50	42	COB+DRV+RPV
89	31	480	31.2	<50	28	DRV+COB+FTC+TAF

EC, Elite Controller; FTC, emtricitabine; TDF, tenofovir; NVP, nevirapine; ATV, atazanavir; 3TC, lamivudine; EFV, efavirenz; ABV, abacavir; RAL, raltegravir; EVG, elvitegravir; DTG, dolutegravir; DRV, darunavir; RPV, Rilpivirine; TAF, tenofovir alafenamida; BIC, Bictegravir; LPV, Lopinavir; /r, boosted with ritonavir; /c, boosted with cobicistat; UNT, untreated; NA: Not Available.

Figure 1

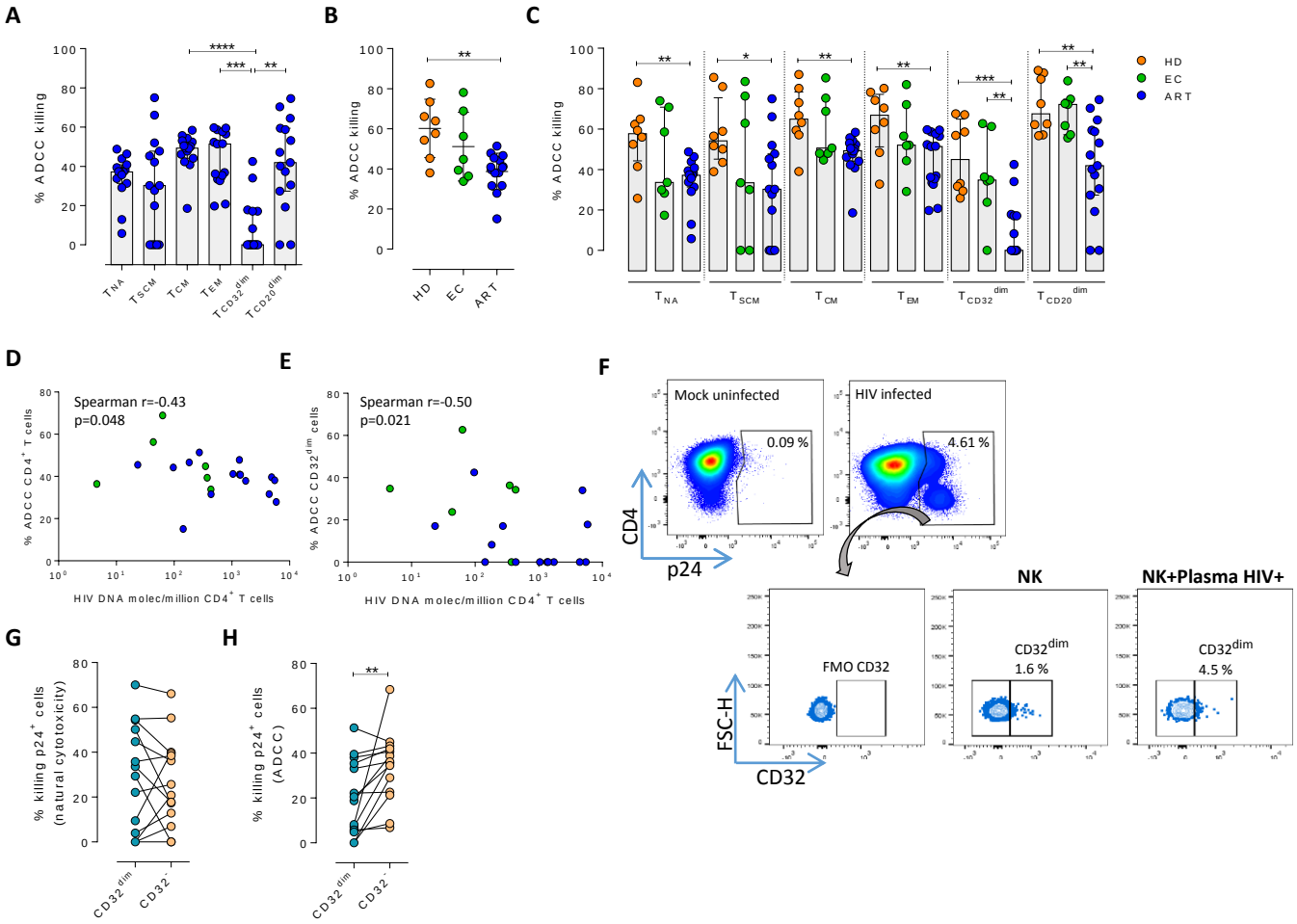

Figure 1. Susceptibility of CD4⁺ T cell subsets to the NK immune response. The susceptibility of different cell subpopulations that compose the HIV-reservoir to Natural Cytotoxicity (NC) and Antibody-Dependent Cell Cytotoxicity (ADCC) mediated by NK cells was measured by performing functional assays. **A)** Percentage of gp120 coated cells killed by ADCC after being exposed to HIV-specific immunoglobulins (Igs) in the presence of NK cells. The intrinsic susceptibility to ADCC was measured in Naïve (T_{NA}), Stem Cell Memory (T_{SCM}), Central Memory (T_{CM}), Effector Memory (T_{EM}), T_{CD32}^{dim}, and T_{CD20}^{dim} subsets. Statistical comparisons were performed using the ANOVA Friedman test. Median with interquartile range is shown. **B)** Percentage of total gp120 coated CD4⁺ T cells from different cohorts of patients killed by ADCC. Healthy donors (HD), Elite Controllers (EC), and antiretroviral treated PLWH (ART). Statistical comparisons were performed using the Mann-Whitney test. Median with interquartile range are shown. **C)** Percentage of cell subsets killed by ADCC in cells from HD, EC, and ART. Statistical comparisons were performed using the Mann-Whitney test. Median with interquartile range is shown. **D-E)** Spearman correlations between the size of the HIV-reservoir measured as total HIV-DNA in samples from ART-suppressed PLWH, and the potency of autologous NK cells to kill (**D**) total CD4⁺ T cells or (**E**) T_{CD32}^{dim} cells by ADCC. **F)** Representative flow cytometry gating strategy used to quantify HIV infection after ex vivo infection with BaL or NL4.3. Fluorescence minus one (FMO) control was used to determine CD32 expression. Cells were infected for 5 days and the frequency of expression of CD32 on HIV-infected cells was measured for each condition. **G)** Percentage of killing by NC of ex-vivo HIV-infected T_{CD32}^{dim} and T_{CD32}^{-} cells mediated by autologous NK cells from ART-treated PLWH (n=14). Killing was calculated by normalizing the proportion of each subset within the p24⁺ fraction in the co-culture condition to the basal condition. **H)** Percentage of ADCC killing of ex vivo HIV-infected T_{CD32}^{dim} and T_{CD32}^{-} cells mediated by autologous NK cells from ART-treated PLWH (n=14). Killing was calculated by normalizing the proportion of each subset within the p24⁺ fraction in the co-culture condition with plasma to the co-culture without plasma. Statistical comparisons were performed using the Wilcoxon matched-pairs signed rank test. *p<0.05; **p<0.01.

Figure 2

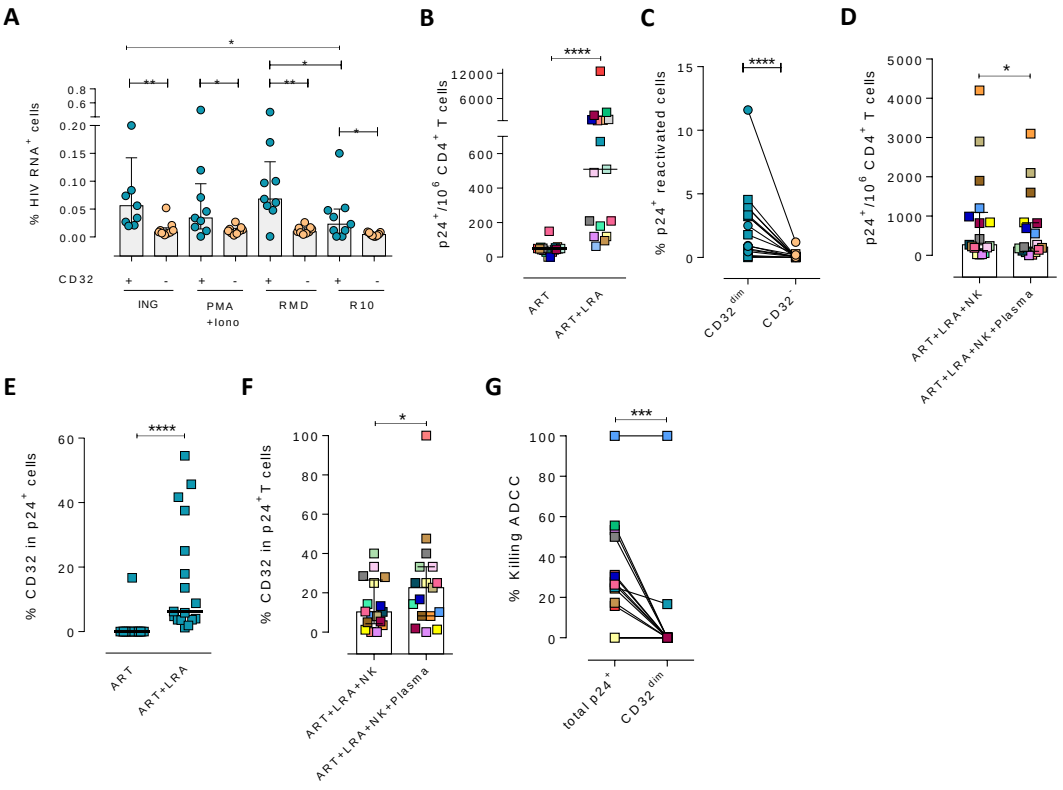

Figure 2. **Expression of HIV in T_{CD32}^{dim} reservoir cells after latency disruption and susceptibility to NK immune responses.** Data from the direct ex vivo reactivation of the natural HIV reservoir in ART-suppressed PLWH. **A)** Percentage of HIV-RNA expressing cells, measured by the RNA FISH-flow assay, within the T_{CD32}^{dim} and T_{CD32}^{-} subsets after viral reactivation with Ingenol, PMA/ionomycin, or romidepsin (n=9). Median with interquartile range is represented. **B)** Percentage of $p24^+$ cells after 18h viral reactivation with PMA/ionomycin (n=17). Each participant is represented by a different color. **C)** Frequency of viral reactivation within the total pool of T_{CD32}^{dim} and T_{CD32}^{-} cells (n=17). **D)** NK killing assays against viral reactivated cells. Number of $p24^+$ cells per million $CD4^+$ T cells after the addition of NK cells only or together with the autologous plasma is shown (n=17). **E)** Percentage of CD32 expression within the total $p24^+$ pool before and after HIV reactivation (n=17). **F)** Percentage of T_{CD32}^{dim} within $p24^+$ cells after HIV reactivation and functional NK-mediated assays (n=17). **G)** Percentage of NK-mediated killing by ADCC of the reactivated T_{CD32}^{dim} or total $p24^+$ cells (n=17). ADCC was calculated as the reduction of $p24^+$ cells after the co-culture with NK and plasma and normalized to the condition with NK cells alone.

Figure 3

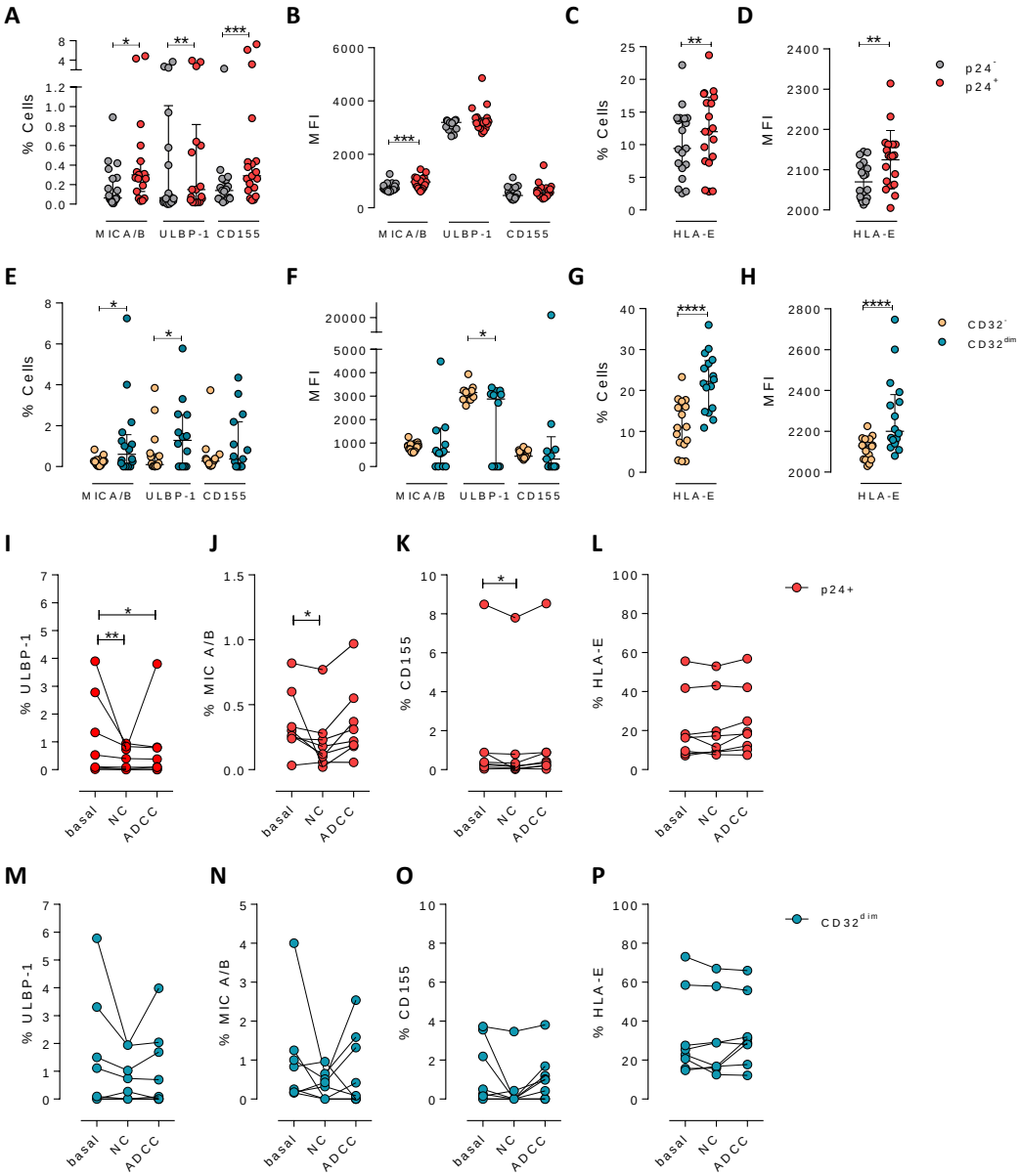

Figure 3. **Expression of NK-ligands in cells resistant to NK-mediated killing.** HIV-infected cells from healthy donors were subjected to NK-killing assays and the percentage of expression of different NK-ligands was measured by flow cytometry in different fractions ($CD32^-$ and $CD32^{dim}$) of infected ($p24^+$) or uninfected ($p24^-$) cells. **A-H)** Expression of NK-ligands before performing the killing assays (n=19): **A)** Percentage of $CD4^+$ T cells expressing MIC A/B, ULBP-1, and CD155. **B)** Mean Fluorescence Intensity (MFI) values for the expression of MIC A/B, ULBP-1, and CD155 on $CD4^+$ T cells. **C)** Percentage of $CD4^+$ T cells expressing the MHC molecule HLA-E. **D)** MFI values for HLA-E expression on $CD4^+$ T cells. **E-H)** Same analyses as A-D but showing HIV-infected $CD32^{dim}$ and $CD32^-$ cells. **I-P)** Expression of NK-ligands on HIV-infected cells not killed by the different NK-killing mechanisms. Natural Cytotoxicity (NC) and Antibody-Dependent Cell Cytotoxicity (ADCC). **I-L)** Expression of NK-ligands on total infected $CD4^+$ T cells before and after NK killing. **M-P)** Expression of NK-ligands on infected $T_{CD32}{}^{dim}$ cells before and after NK killing. All graphs show median with interquartile range and the statistical comparisons were performed using the Wilcoxon matched-pairs signed rank test.*p<0.05; **p<0.01; ***p<0.001; ****p<0.0001.

Figure 4

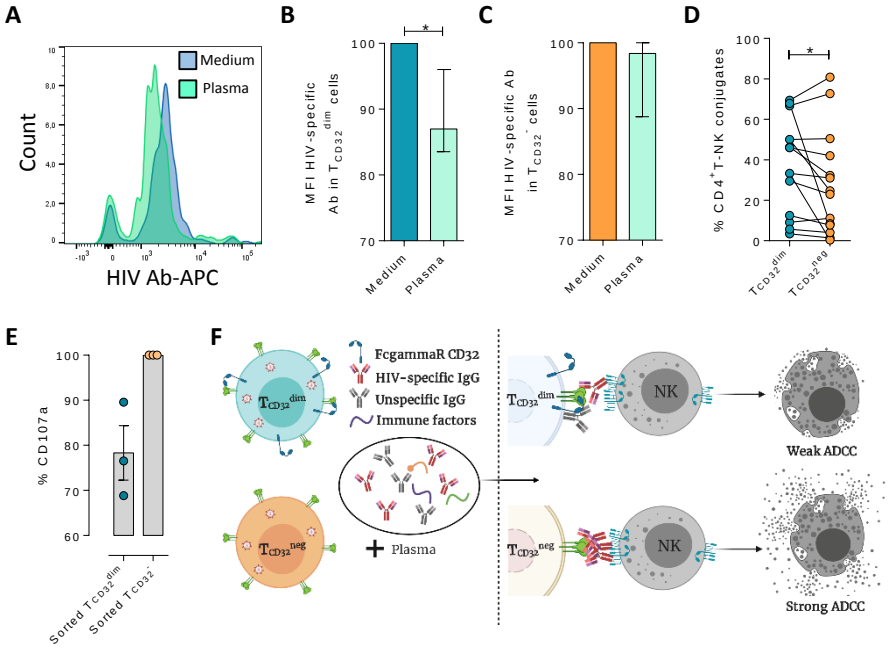

Figure 4. Reduced binding of HIV-specific antibodies to T_{CD32}^{dim} cells and the effect on NK degranulation. The binding capability of the HIVgp120-specific IgG A32, an antibody (Ab) labelled with allophycocyanin (APC), to gp120-coated T_{CD32}^{dim} and T_{CD32}^{-} cells from healthy donors, before and after incubation with plasma containing non-HIV specific IgGs, was measured by flow cytometry (n=7). Percentage of the Mean Fluorescence Intensity (MFI) signal, normalized to the medium, for $A32^{+}$ cells after plasma addition is shown in **A)** Representative histogram of $A32^{+}$ T_{CD32}^{dim} cells, **B)** T_{CD32}^{dim} and **C)** T_{CD32}^{-} cells. **D)** Percentage of cell conjugates between ex vivo HIV-infected T_{CD32}^{dim} or T_{CD32}^{-} and NK cells after performing ADCC assays (n=14). **E)** Percentage of NK degranulation (CD107a marker) in cell conjugates with sorted T_{CD32}^{dim} or T_{CD32}^{-} coated with gp120 HIV protein and incubated with plasma HIV^{+}, after a 4h ADCC activation assay (n=3). Values are normalized to the $CD32^{-}$ population. **F)** Schematic illustration of the impaired ADCC response against T_{CD32}^{dim} cells. Graphs show median with range and statistical comparisons were performed using Wilcoxon matched-pairs signed rank test. *p<0.05.

Figure 5

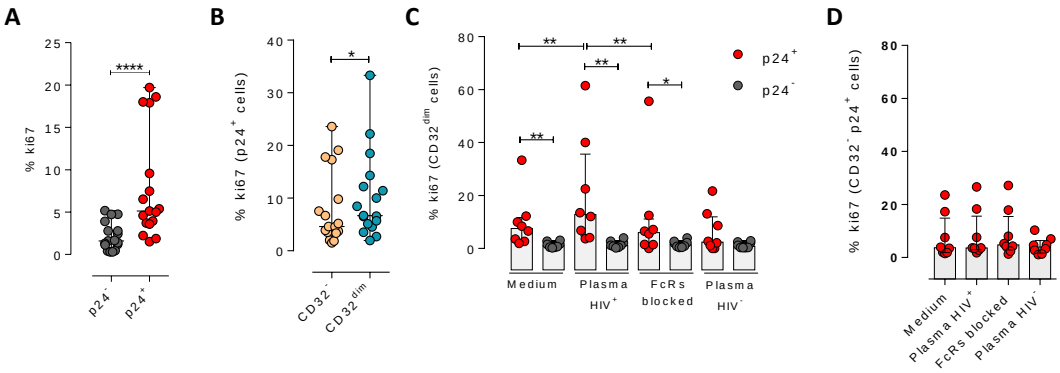

Figure 5. **Immune complexes engagement with CD32 induces proliferation in HIV-infected CD32^{dim} cells.** Cells from healthy donors were infected with the viral strain HIV_{BaL} and 5 days post-infection Ki67 expression was measured by flow cytometry. **A)** Expression of the proliferation marker Ki67 in uninfected or ex-vivo HIV-infected $CD4^+$ T cells. Median and ranges are shown (n=17). **B)** Percentage of $Ki67^+$ cells in HIV-infected T_{CD32}^{dim} and T_{CD32}^{-} subsets are shown (n=17). Median and ranges are shown. **C)** Percentage of Ki67 expression on T_{CD32}^{dim} cells after immune complexes engagement (Plasma HIV^+). Medium alone, FcRs blockers and plasma from an HIV-negative individual were included as controls. Median with interquartile range is shown (n=8). **D)** Percentage of Ki67 expression on HIV-infected T_{CD32}^{-} cells incubated under the same experimental conditions as shown in **C**. Median with interquartile range is represented (n=8). Statistical comparisons consisted of the Wilcoxon matched-pairs signed rank test.*p<0.05; **p<0.01; ***p<0.001; ****p<0.0001.

Figure 6

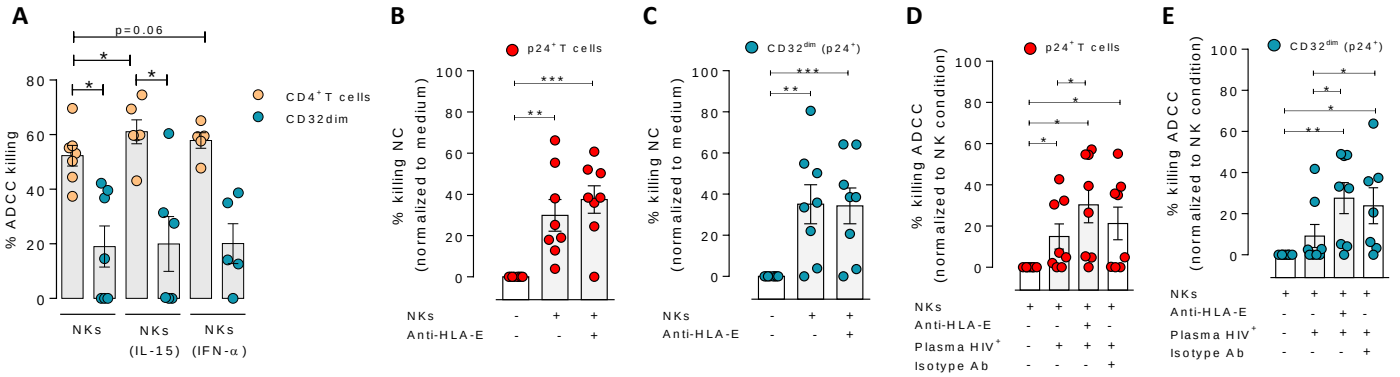

Figure 6. **Effect of IL-15, IFN-α and anti-HLA-E antibody in the NK function.** CD4⁺ T cells from ART-suppressed participants, either coated with a gp120 recombinant protein (A) or, ex vivo infected with $HIV_{NL4.3}$ (B to E), were subjected to Natural Cytotoxicity (NC) (NK condition) and ADCC (NK + plasma) assays in the presence of cytokines or blocking antibodies. **A)** Percentage of ADCC killing of HIVgp120-coated CD4⁺ T cells by autologous NK cells after treatment with IL-15 or IFN-α. Mean with SEM is represented. **B-E)** Graphs showing the percentage of reduction in HIV-infected cells after using anti-HLA-E antibodies or isotype controls in NC and ADCC functional assays (n=8), in total p24⁺ CD4⁺ T cells (**B** and **D**) and in T_{CD32}^{dim} (p24⁺) cells (**C** and **E**). Mean with SEM is represented. Statistical comparisons consisted of the One Sample T test or the Wilcoxon matched-pairs signed rank test.*p<0.05; **p<0.01.

Figure S1

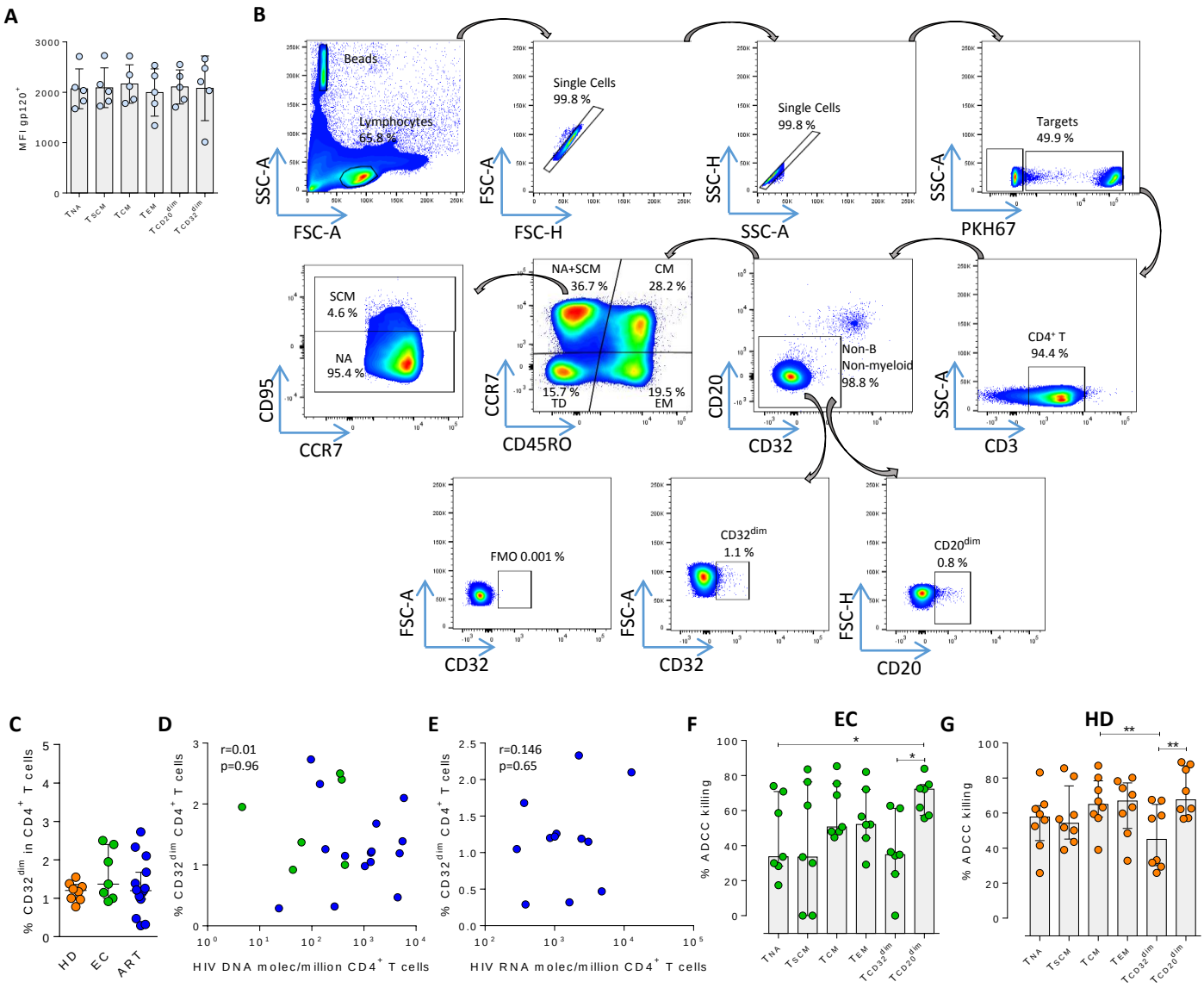

Figure S1. Gp120 cell coating efficiency, gating strategy for the NK-killing assays, and percentages of ADCC killing in elite controllers (EC), and healthy donors (HD). A) Cell coating with recombinant gp120 HIV protein. Detection was performed by flow cytometry using the anti-gp120 antibody A32, and a FITC-labelled anti-human secondary antibody. Mean Fluorescence Intensity (MFI) values are shown. **B)** Gating strategy used to identify cell killing after the ADCC assay in the different cell subsets. Cell doublets were excluded by forward and side scatter signals and B and myeloid cells discarded based on their high expression of CD20 and CD32. Beads for absolute cell counting were included to calculate ADCC killing by measuring the disappearance of cells in each cell subset. **C)** Frequency of expression measured by flow cytometry of CD32 on $CD4^+$ T cells from healthy donors (HD, n=8), Elite controllers (EC, n=7) and ART-treated and virologically-suppressed PLWH (ART, n=15). Median with interquartile range are shown. Statistical comparisons were performed using the Mann-Whitney test. ***p<0.001; ****p<0.0001. **D-E)** Correlations of the HIV-reservoir size and CD32 expression. Spearman correlations are shown in samples from HIV-infected individuals. ART-treated and EC are shown in blue and green dots, respectively. **D)** Spearman correlation between the total HIV DNA reservoir size and the frequency of expression of CD32 in $CD4^+$ T cells. ART-treated and EC are shown in blue and green dots, respectively. **E)** Spearman correlation between HIV RNA levels in $CD4^+$ T cells and the frequency of expression of CD32 in $CD4^+$ T cells. **F-G)** Intrinsic susceptibility to NK-mediated ADCC of Naïve (T_{NA}), Stem Cell Memory (T_{SCM}), Central Memory (T_{CM}), Effector Memory (T_{EM}), T_{CD32}^{dim} and T_{CD20}^{dim} subsets in **F)** EC, and **G)** HD. Median with interquartile range is shown. Statistical comparisons were performed using the ANOVA Friedman test. *p<0.05; **p<0.01.

Figure S2

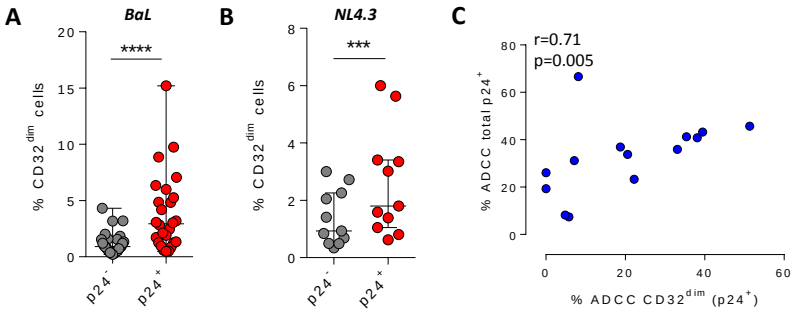

Figure S2. Percentage of CD32 expression on uninfected cells ($p24^-$) and HIV-infected cells ($p24^+$) with BaL (n=26) in (**A**) or with NL4.3 (n=11) in (**B**) after 5 days of infection. Median with interquartile range are shown. Statistical analyses consisted of the Wilcoxon matched-pairs signed rank test. **C)** Spearman correlation between the percentage of ADCC-killing of the total HIV-infected $CD4^+$ T cells and the percentage of ADCC-killing of the T_{CD32}^{dim} subset is shown.

Figure S3

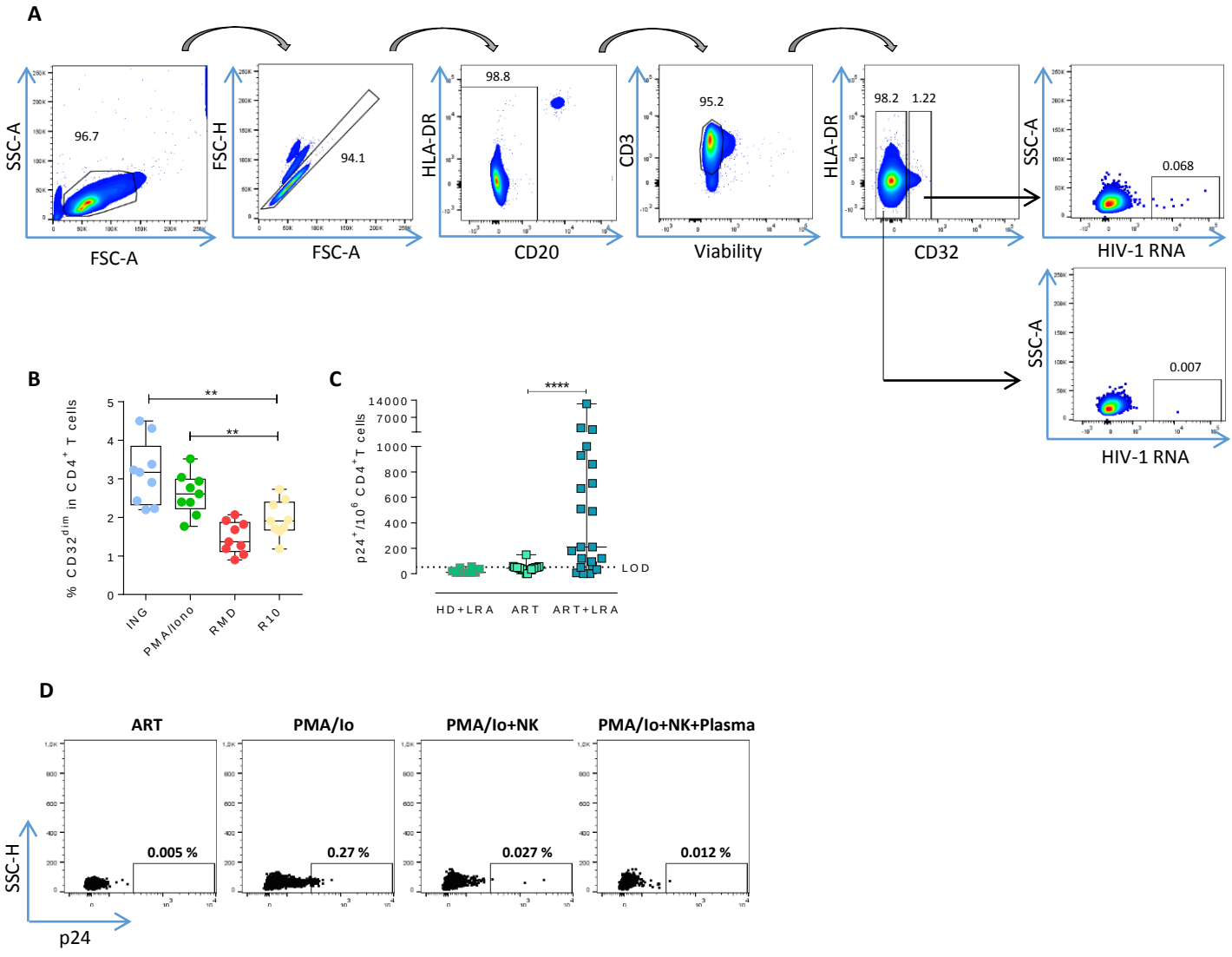

Figure S3. Expression of HIV-RNA and viral protein p24 in T_{CD32}^{dim} reservoir cells after viral reactivation. A) Flow cytometry gating strategy used for the identification of T_{CD32}^{dim} cells expressing HIV-RNA after the RNA FISH-flow protocol. **B)** Percentage of CD32 expression within the total $CD4^+$ T cells before and after LRA treatment, using samples from ART-suppressed PLWH subjected to RNA FISH-flow assay. Statistical comparisons consisted of the Wilcoxon matched-pairs signed-rank test. **p<0.01. **C)** $p24^+$ cells in samples from ART-suppressed individuals at baseline and after viral reactivation with PMA/ionomycin (LRA). The limit of detection is set up at 53 copies/million cells calculated by the formula 3*SD of the mean percentage of p24+ cells detected in healthy donor (HD) samples. **D)** Representative flow cytometry plots of viral reactivation levels (measured as $p24^+$ cells) after LRA treatment and NK functional assays.

Figure S4

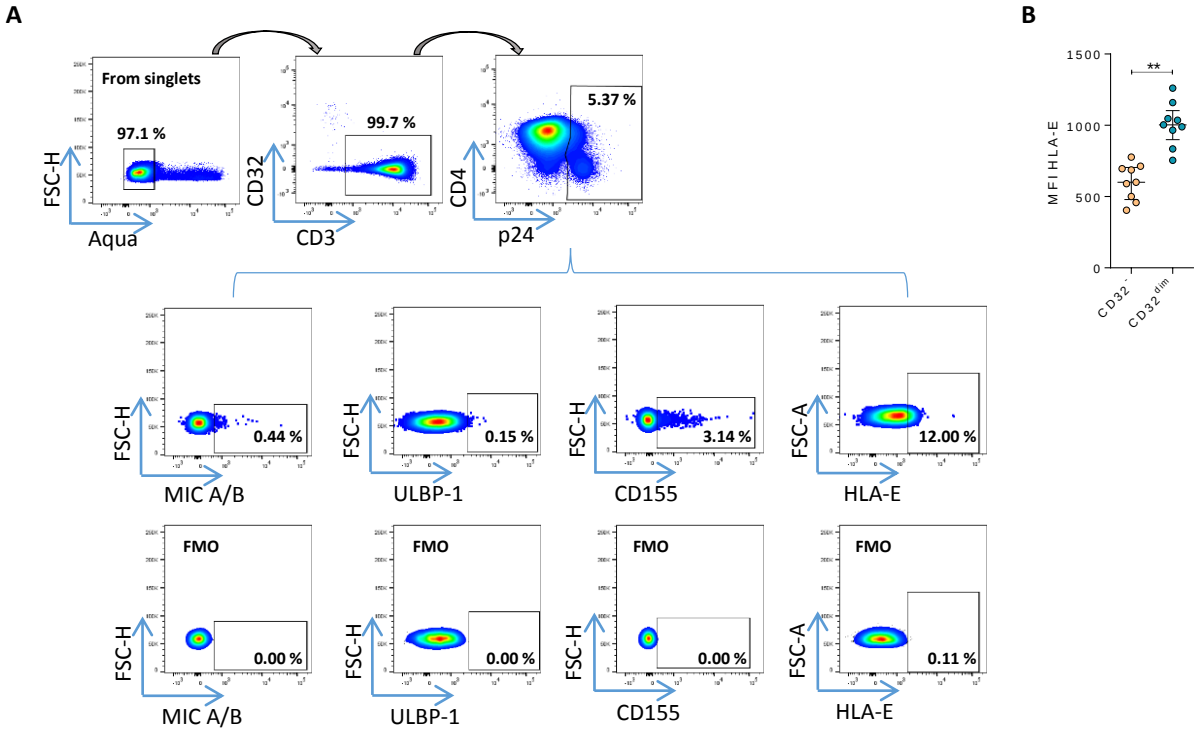

Figure S4. NK-ligands on HIV-infected cells. A) Representative flow cytometry gating strategy used to quantify the expression of MIC A/B, ULBP-1, CD155, and HLA-E ligands on HIV-infected cells after ex vivo infection. FMO controls are also shown. **B)** Mean Fluorescence Intensity (MFI) values of HLA-E expression on $CD4^+$ T cells in the absence of HIV infection. Median with interquartile range is shown. Statistical comparison consisted of the Wilcoxon matched-pairs signed rank test. **$p<0.01$.

Figure S5

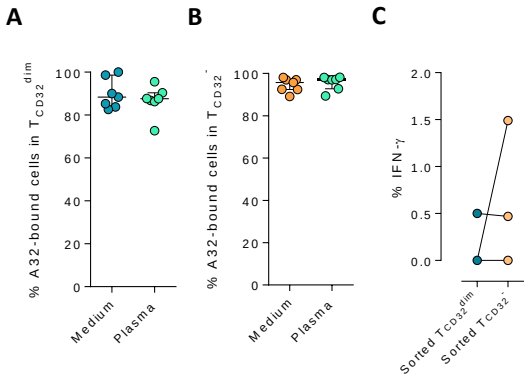

Figure S5. Binding of A32 to T cells and percentage of IFN-γ in cell conjugates. The binding capability of the A32 HIV-specific antibody (APC-labeled) to gp120-coated T_{CD32}^{dim} and T_{CD32}^{-} before and after incubation with plasma containing non-HIV specific IgGs, was measured by flow cytometry. **A)** Percentage of $A32^{+}$ T_{CD32}^{dim} cells. **B)** Percentage of $A32^{+}$ T_{CD32}^{-} cells. **C)** Percentage of IFN-γ^{+} NK cells in cell conjugates with sorted T_{CD32}^{dim} and T_{CD32}^{-} cells after ADCC assays. Statistical comparisons were performed using the Wilcoxon matched-pairs signed rank test. *$p<0.05$.